


NACA TN 3005

TECH LIBRARY KAFB, NM  
0066125



# NATIONAL ADVISORY COMMITTEE FOR AERONAUTICS

TECHNICAL NOTE 3005

HEAT TRANSFER AND SKIN FRICTION BY AN INTEGRAL METHOD  
IN THE COMPRESSIBLE LAMINAR BOUNDARY LAYER WITH  
A STREAMWISE PRESSURE GRADIENT

By Ivan E. Beckwith

Langley Aeronautical Laboratory  
Langley Field, Va.



Washington  
September 1953

AFMDC  
TECHNICAL LIBRARY  
AFL 2811

## TECHNICAL NOTE 3005

HEAT TRANSFER AND SKIN FRICTION BY AN INTEGRAL METHOD  
IN THE COMPRESSIBLE LAMINAR BOUNDARY LAYER WITH  
A STREAMWISE PRESSURE GRADIENT

By Ivan E. Beckwith

## SUMMARY

A simplified method has been developed for the calculation of heat transfer and skin friction in the compressible laminar boundary layer with an arbitrary Prandtl number near unity and an arbitrary streamwise pressure gradient and wall temperature distribution. By comparison of numerical results with some exact solutions, the method is shown to give accurate results for the case of boundary-layer cooling when a certain fifth-degree polynomial is used for the thermal profile. The use of this polynomial also results in recovery factors which are accurate to within a few percent on both the flat plate and the circular cylinder normal to the flow.

The method may be extended to calculation of heat transfer with equilibrium dissociation provided the wall temperature is below dissociation temperatures. A numerical example for the heat transfer in the stagnation region of a blunt body shows that equilibrium dissociation probably has little effect on the actual heat-transfer rate.

The effect of lateral radius of curvature on skin friction and heat transfer is investigated for compressible flow. The approximate method used herein indicates that this effect is negligible unless the square root of the wall Reynolds number (based on body length and the gas properties evaluated at the wall) is of the order of or less than 100 times the body fineness ratio.

## INTRODUCTION

The calculation of the laminar boundary layer with an arbitrary pressure gradient is as yet impractical except by the Von Kármán-Pohlhausen integral methods. In general, these methods are somewhat tedious to apply; however, recent improvements have reduced the calculations with zero heat transfer to a simple quadrature of certain

functions of the known free-stream velocity and temperature distributions. These various refinements which both simplify and improve the accuracy of the basic integral methods have been developed by Thwaites (ref. 1), Truckenbrodt (ref. 2), and others. (See discussion in ref. 3.) Rott and Crabtree (ref. 3) have extended the method of Thwaites to compressible flow with zero heat transfer and a Prandtl number of unity. Morduchow and Clarke (ref. 4) have also treated the problem of compressible flow with zero heat transfer and a Prandtl number of unity by a different approach which, for practical purposes, gives results of equal accuracy and equal simplicity of calculation. The method of reference 4 results in velocity profiles of sufficient accuracy for stability calculations, whereas the methods of references 1 and 3 cannot be used for this purpose.

If the heat transfer is included as another unknown, the problem is more complicated, particularly for an arbitrary surface temperature distribution. Dienemann (ref. 5) has shown that the calculation with heat transfer in incompressible flow can be simplified by application of the Holstein-Bohlen version of the Von Karman-Pohlhausen method. For an isothermal surface and a Prandtl number of unity, Morduchow (ref. 6) uses assumptions similar to those in reference 4 to simplify the problem of heat transfer on a sweat-cooled wall in compressible flow. The work of reference 6 is an extension (to include a normal velocity at the wall) of the method of Kalikhman (ref. 7) which also gives detailed results only for a Prandtl number of unity but is not restricted to an isothermal surface. The stagnation-temperature profiles are assumed as fourth-degree polynomials in the normal distance in both references 6 and 7.

Recent theoretical and experimental work (for example, refs. 8 to 11) has indicated that boundary layers in high-speed flow may be laminar at relatively large Reynolds numbers under conditions of boundary-layer cooling and favorable pressure gradients. Therefore, the accurate calculation of heat transfer and skin friction under these conditions is of considerable interest. The purpose of the present paper is to trace the development of a method by which these calculations can be made with relative simplicity. The present method, which is essentially a modification of Kalikhman's method (ref. 7), uses an arbitrary Prandtl number near unity and several different stagnation-temperature profiles in conjunction with a fourth-degree velocity profile. The principal simplifying assumptions and procedures are (1) equal thermal and velocity boundary-layer thicknesses, (2) linear viscosity-temperature relation, (3) use of the first coefficient in the polynomial for the stagnation-temperature profile as one of the unknowns in the final solution of the momentum and energy equations, and (4) application of the Holstein-Bohlen method to avoid the use of the second derivative of the stream velocity. The results in the form of heat-transfer and skin-friction coefficients and recovery factors are then compared with exact

solutions for the nonisothermal flat plate (ref. 12), stagnation flow (refs. 13 and 14), and flow over a cylinder (ref. 15). The recovery factors on a cylinder are compared with the supersonic data of Eber (ref. 16).

The effects of equilibrium dissociation (as given by Moore for the flat plate in ref. 17) on the heat transfer at a surface cooler than about  $2,000^{\circ}\text{R}$  in the presence of a velocity gradient are also considered in the present analysis. A numerical example is then given that shows the approximate effect of dissociation in the stagnation region of a blunt-nose body.

After the present investigation was completed, the author learned of a paper by Paul A. Libby and Morris Morduchow of the Polytechnic Institute of Brooklyn who, in some instances, used procedures and assumptions similar to those of the present analysis. Their method used a sixth-degree polynomial for the velocity profile and a seventh-degree polynomial for the stagnation-temperature profile. Although the sixth-degree velocity profile is probably necessary for stability calculations, the seventh-degree thermal profile, as indicated by this analysis, in some cases gives less accurate results than a simpler fourth- or fifth-degree thermal profile.

#### SYMBOLS

$A_1, A_2, \dots$	coefficients of velocity profile (eq. (12))
$a_0, a_1, \dots, a_n$	constants in expression for wall temperature (eq. (47))
$B_1, B_2, \dots$	coefficients for stagnation-enthalpy profile $\bar{t}$ (eq. (16))
$b_1, b_2, \dots$	coefficients for the density function (eq. (26))
$C_f$	mean skin-friction coefficient
$C_w = \frac{\mu_w \rho_w}{\mu_1 \rho_1}$	
$c_f$	local skin-friction coefficient
$c_p$	specific heat at constant pressure
$F_r$	"local" recovery factor (eq. (62))
$F_r'$	"local free stream" recovery factor (eq. (63))

$$f_w = \frac{1}{\rho_w \mu_w} \int_0^x \mu_w \rho_w dx$$

H stagnation enthalpy,  $h + \frac{u^2}{2}$

$$\bar{H} = \frac{\Phi}{\theta}$$

h static enthalpy

$K_0, K_1, \dots$  constants (eq. (75))

k conductivity

L characteristic dimension

M Mach number

m constant,  $\frac{1}{2} - \frac{37}{1260\alpha_1\sigma}$

Nu Nusselt number

n degree of polynomial for wall temperature (eq. (47))

p pressure

q local convective heat-transfer rate

$$R_{0L} = \frac{\rho_0 u_0 L}{\mu_0}$$

$$R_{1L} = \frac{\rho_1 u_1 L}{\mu_1}$$

$$R_{\infty L} = \frac{\rho_{\infty} u_{\infty} L}{\mu_{\infty}}$$

r radial distance from axis for cylindrical coordinates

T absolute temperature

$T_e$  wall temperature for zero heat transfer

$$\bar{T}_W = \frac{T_W}{T_1^*}$$

$T^*$  stagnation temperature,  $T + \frac{u^2}{2c_p}$

$$t_e = \frac{T_e}{T_1^*}$$

$$\bar{t} = \frac{t^*}{t_1^*} = \frac{H - H_W}{H_1 - H_W}$$

$t^* = H - H_W = H - c_{pW}T_W$  for  $T_W < 2,000^\circ \text{R}$

$u$  velocity in x-direction

$v$  velocity in y-direction

$w$  velocity ratio,  $u/u_1$

$x, y$  boundary-layer coordinates;  $y = 0$  is body surface

$$\bar{x} = \frac{x}{L}$$

$Y_n'(0)$  heat-transfer parameter for nonisothermal flat plate in notation of ref. 12

$Z$  computation parameter defined by equation (67)

$\alpha, \alpha_1, \alpha_2 \dots$  constants in energy-loss thickness (eq. (35)), numerical values given in table I

$$\beta_W = \cos^{-1} \frac{r - r_W}{y}$$

$\gamma$  ratio of specific heats (approximately 1.40 for air)

$\Delta$  nominal boundary-layer thickness in  $x, \eta$  plane

$$\Delta^* = \Delta \int_0^1 (1 - \bar{t}) d\eta^* \quad (\text{eq. (25)})$$

$\delta^*$	displacement thickness in $x, \eta$ plane (eq. (23))
$\eta$	Dorodnitsyn variable, $\int_0^y \frac{\rho}{\rho^*_1} dy$
$\eta_r$	modified Dorodnitsyn variable for slender body (eq. (A7))
$\eta^* = \frac{\eta}{\Delta}$	
$\eta^*_r = \frac{\eta_r}{\Delta}$	
$\theta$	momentum-loss thickness in $x, \eta$ plane (eq. (22))
$\bar{\theta} = \frac{\theta}{L}$	
$\lambda$	modified Pohlhausen parameter (eq. (15))
$\lambda'$	modified Pohlhausen parameter for slender body (eq. (A14))
$\mu$	viscosity
$\xi = \frac{x}{r_w} \sqrt{\frac{\mu_w}{\rho_w u_{1x}}}$	
$\xi' = \frac{x}{r_w} \sqrt{\frac{\mu_1}{\rho_1 u_{1x}}}$	
$\rho$	mass density
$\rho^*$	stagnation density
$\sigma$	Prandtl number, $c_p \mu / k$
$\tau$	local shear stress
$\phi$	energy-loss thickness integral in $x, \eta$ plane (eq. (24))
$\bar{\phi} = \frac{\phi}{L}$	

$\Omega$  density integral,  $\Delta \int_0^1 \left( \frac{\rho_1}{\rho} - \frac{u}{u_1} \right) d\eta^*$

Subscripts:

1 local free stream just "outside" boundary layer  
 $\infty$  free stream at infinity  
 w wall values  
 B or o some constant reference quantity  
 p flat-plate values (zero pressure gradient)

BASIC EQUATIONS

In the following discussion, the boundary-layer equations and their integrals are given in their most general form where the only restrictions are that the gas is a continuum and that the boundary layer is thin compared with a characteristic dimension of the body, that is, the characteristic Reynolds number of the body is large. For application to dissociation, two additional restrictions are used. These restrictions are as follows: the assumption of equilibrium dissociation throughout so that no rate process terms are required in the energy equation (see ref. 17), and the restriction that all wall temperatures are less than about 2,000<sup>o</sup> R. The two-dimensional equations only are considered herein since the results may be extended to axisymmetric flow by Mangler's transformation (ref. 18) except where conditions are such that the boundary-layer thickness is of the order of the lateral radius of the body. The effects of these conditions are investigated in detail in the appendix for a slender cylinder aligned parallel to the flow.

The boundary-layer equations for steady flow are written as follows:

Momentum equation:

$$\rho u \frac{\partial u}{\partial x} + \rho v \frac{\partial u}{\partial y} = - \frac{\partial p}{\partial x} + \frac{\partial}{\partial y} \left( \mu \frac{\partial u}{\partial y} \right) \quad (1)$$

$$0 = \frac{\partial p}{\partial y} \quad (2)$$



Continuity equation:

$$\frac{\partial}{\partial x} \rho u + \frac{\partial}{\partial y} \rho v = 0 \quad (3)$$

Energy equation:

$$\rho u \frac{\partial h}{\partial x} + \rho v \frac{\partial h}{\partial y} = u \frac{\partial p}{\partial x} + \frac{\partial}{\partial y} \left( k \frac{\partial T}{\partial y} \right) + \mu \left( \frac{\partial u}{\partial y} \right)^2 \quad (4)$$

or in terms of the stagnation enthalpy  $H = h + \frac{u^2}{2}$ ,

$$\rho u \frac{\partial H}{\partial x} + \rho v \frac{\partial H}{\partial y} = \frac{\partial}{\partial y} \left( \mu \frac{\partial H}{\partial y} \right) + \frac{\partial}{\partial y} \left[ \mu \frac{\partial h}{\partial y} \left( \frac{1}{\sigma} - 1 \right) \right] \quad (5)$$

where the Prandtl number  $\sigma$  is defined as

$$\sigma = \frac{\mu}{k} c_p = \frac{\mu}{k} \frac{dh}{dT}$$

Integration of equation (1) across the boundary layer (with the conditions  $u = v = 0$  at  $y = 0$  and  $u = u_1$  at  $y = \infty$ ) and the use of equations (2) and (3) result in

$$\begin{aligned} \frac{d}{dx} \int_0^{\infty} \left( \frac{u}{u_1} - \frac{u^2}{u_1^2} \right) \frac{\rho}{\rho^*_1} dy + \left[ 2 \int_0^{\infty} \left( \frac{u}{u_1} - \frac{u^2}{u_1^2} \right) \frac{\rho}{\rho^*_1} dy + \right. \\ \left. \int_0^{\infty} \left( \frac{\rho_1}{\rho} - \frac{u}{u_1} \right) \frac{\rho}{\rho^*_1} dy \right] \frac{1}{u_1} \frac{du_1}{dx} = \frac{\mu_w}{u_1 \rho^*_1} \left( \frac{\partial u}{\partial y} \right)_w \end{aligned} \quad (6)$$

where Bernoulli's equation  $\frac{dp}{dx} = -\rho_1 u_1 \frac{du_1}{dx}$  has been used for the pressure gradient, and the free-stream stagnation density  $\rho^*_1$  is assumed constant along the edge of the boundary layer.

Similarly, integration of equation (5) and the use of equation (3) result in

$$\frac{d}{dx} \int_0^{\infty} \frac{u}{u_1} \left(1 - \frac{t^*}{t^*_1}\right) \frac{\rho}{\rho^*_1} dy + \left( \frac{1}{u_1} \frac{du_1}{dx} - \frac{1}{t^*_1} \frac{dt^*_1}{dx} \right) \int_0^{\infty} \frac{u}{u_1} \left(1 - \frac{t^*}{t^*_1}\right) \frac{\rho}{\rho^*_1} dy =$$

$$\frac{\mu_w}{\sigma_w \rho^*_1 u_1} \left( \frac{\partial}{\partial y} \frac{t^*}{t^*_1} \right)_w \quad (7)$$

where the free-stream stagnation enthalpy  $H_1$  is assumed constant. Transformation to the Dorodnitsyn variable  $\eta$  defined as

$$\eta = \int_0^y \frac{\rho}{\rho^*_1} dy \quad (8)$$

results in

$$\frac{d}{dx} \int_0^{\infty} \left( \frac{u}{u_1} - \frac{u^2}{u_1^2} \right) d\eta + \left[ 2 \int_0^{\infty} \left( \frac{u}{u_1} - \frac{u^2}{u_1^2} \right) d\eta + \int_0^{\infty} \left( \frac{\rho_1}{\rho} - \frac{u}{u_1} \right) d\eta \right] \frac{1}{u_1} \frac{du_1}{dx} =$$

$$\frac{\mu_w \rho_w}{u_1 (\rho^*_1)^2} \left( \frac{\partial}{\partial \eta} \frac{u}{u_1} \right)_w \quad (9)$$

and

$$\frac{d}{dx} \int_0^{\infty} \frac{u}{u_1} \left(1 - \frac{t^*}{t^*_1}\right) d\eta + \left( \frac{1}{u_1} \frac{du_1}{dx} - \frac{c_{p_w}}{t^*_1} \frac{dt^*_1}{dx} \right) \int_0^{\infty} \frac{u}{u_1} \left(1 - \frac{t^*}{t^*_1}\right) d\eta =$$

$$\frac{\mu_w \rho_w}{\sigma_w (\rho^*_1)^2 u_1} \left( \frac{\partial}{\partial \eta} \frac{t^*}{t^*_1} \right)_w \quad (10)$$

This derivation of equations (9) and (10) follows that of reference 7.

## VELOCITY AND ENTHALPY PROFILES

The usual procedure in the Von Kármán-Pohlhausen integral methods is to assume the velocity profile as a polynomial in the normal distance parameter  $\eta$ . The fourth-degree polynomial is sufficiently accurate for most engineering purposes except stability investigations and prediction of separation as shown, for example, in references 4 and 19 for zero heat transfer. There is no way of knowing beforehand whether the same conclusions are valid in the presence of heat transfer. However, since the present analysis is concerned mainly with the effect on the heat transfer of different enthalpy or temperature profiles, the fourth-degree polynomial for the velocity profile is used throughout for simplicity in calculation.

The velocity profile is then written

$$\frac{u}{u_1} = w = A_1\eta^* + A_2(\eta^*)^2 + A_3(\eta^*)^3 + A_4(\eta^*)^4 \quad (11)$$

The usual boundary values are specified at the edge of the boundary layer such that, at  $\eta^* = 1$ ,

$$w = 1$$

$$\frac{\partial w}{\partial \eta^*} = 0$$

$$\frac{\partial^2 w}{\partial (\eta^*)^2} = 0$$

From these boundary conditions and equation (11), the following relations are obtained:

$$\left. \begin{aligned} A_1 &= \left( \frac{\partial w}{\partial \eta^*} \right)_w = \frac{12 + \lambda}{6} \\ A_3 &= \frac{1}{6} \left[ \frac{\partial^3 w}{\partial (\eta^*)^3} \right]_w = \frac{3\lambda - 12}{6} \\ A_4 &= \frac{6 - \lambda}{6} \\ \lambda &= -2A_2 = - \left[ \frac{\partial^2 w}{\partial (\eta^*)^2} \right]_w \end{aligned} \right\} \quad (12)$$

In order to simplify the remaining boundary condition, it is convenient to introduce the assumptions that, in the immediate vicinity of the surface only,

$$\mu = \frac{\mu_w}{T_w} T \quad (13)$$

and

$$\rho = \rho_w T_w \frac{1}{T} \quad (14)$$

These assumptions should not be unduly restrictive so long as the surface temperature is less than 2,000° R (that is, well below the dissociation temperature of the gas) since  $\mu_w$  may be evaluated as accurately as desired to correspond to  $T_w$ . Evaluating equation (1) at  $y = 0$  and using equations (13), (14), (8), and (12) give the required expression for  $\lambda$  as

$$\lambda = \frac{\rho_1}{\mu_w} \left( \frac{\rho^*_{1}}{\rho_w} \right)^2 \frac{du_1}{dx} \Delta^2 \quad (15)$$

In a similar manner the stagnation enthalpy profile is written as a general polynomial in  $\eta^*$ ,

$$\frac{t^*}{t^*_1} = \bar{t} = B_1 \eta^* + B_2 (\eta^*)^2 + B_3 (\eta^*)^3 + B_4 (\eta^*)^4 + \dots \quad (16)$$

where up to six terms will be used. The edge boundary conditions are taken as two or more asymptotic requirements at  $\eta^* = 1$  and are

$$\left. \begin{aligned} \bar{t} &= 1 \\ \frac{\partial^n \bar{t}}{\partial (\eta^*)^n} &= 0 \end{aligned} \right\} \quad (17)$$

where  $n$  is a positive integer.

Equations (17) imply the assumption that the thermal and velocity boundary layers are always of equal thickness. In contrast to this assumption, Morduchow (ref. 6) has assumed that the thermal and velocity layers are always in the same ratio on any particular body. The results of the exact solution of Brown and Donoughe (ref. 13) of wedge-type flows with Prandtl number of 0.7, however, indicate that the nominal value of this ratio is approximately unity for a wide range of pressure gradients and wall temperatures. Furthermore, the computations of Levy (ref. 20) show that, even for a Prandtl number as large as 5, the thermal boundary-layer thickness can be considered as roughly 70 percent of the velocity boundary-layer thickness because of the asymptotic nature of the profiles. As will be shown subsequently, the results of the present analysis indicate that the assumption of equations (17) gives good accuracy when used in a certain combination with the wall boundary conditions for equation (16).

These wall boundary conditions are determined from equation (5) and its first derivative with respect to  $y$  evaluated at  $y = 0$ . With the use of equations (13) and (14) and the transformation formulas from equation (8), the wall boundary conditions for the enthalpy profile may be written as

$$\left(\frac{\partial^2 t^*}{\partial \eta^2}\right)_w = (1 - \sigma_w) \left(\frac{\partial u}{\partial \eta}\right)_w^2 \quad (18)$$

and

$$\left(\frac{\partial^3 t^*}{\partial \eta^3}\right)_w = \sigma_w \frac{\rho_w}{\mu_w} c_{p_w} \left(\frac{\rho^*_1}{\rho_w}\right)^2 \left(\frac{\partial u}{\partial \eta}\right)_w \frac{dT_w}{dx} + 3(1 - \sigma_w) \left(\frac{\partial u}{\partial \eta}\right)_w \left(\frac{\partial^2 u}{\partial \eta^2}\right)_w \quad (19)$$

where the additional assumptions have been used that  $\sigma$  and  $c_p$  are constant very near the wall. By using equations (12) and the assumption that the thermal and velocity boundary layers are of equal thickness, equations (18) and (19) can be written as

$$2B_2 = \frac{\partial^2 \bar{t}}{\partial (\eta^*)^2} = (1 - \sigma_w) \frac{u_1^2}{t^*_1} \left(\frac{12 + \lambda}{6}\right)^2 \quad (20)$$

$$6B_3 = \frac{\partial^3 \bar{t}}{\partial (\eta^*)^3} = \frac{u_1}{t^*_1} \lambda \frac{12 + \lambda}{6} \left[ \sigma_w c_{p_w} \frac{\rho_w}{\rho_1} \frac{dT_w/dx}{du_1/dx} - 3(1 - \sigma_w) u_1 \right] \quad (21)$$

(Eq. (15) has also been used in eq. (19).)

## GENERAL METHOD OF SOLUTION

The general procedure for the solution of equations (9) and (10) consists of using two or more of the asymptotic requirements (eqs. (17)) and one or both of the wall conditions (eqs. (20) and (21)) such as to specify all but one of the coefficients of the stagnation enthalpy profile in terms of  $\lambda$  and the known external flow. The remaining coefficient of equation (16), say  $B_1$ , and  $\lambda$  will then be the two unknown quantities to be found from the simultaneous solution of equations (9) and (10).

Before the solution can be effected, explicit expressions for the integrals of the velocity and enthalpy profiles are required. Thus, as usual for the fourth-degree velocity profile, the momentum-loss thickness integral is

$$\frac{\theta}{\Delta} = \int_0^1 (w - w^2) d\eta^* = \frac{1}{315} \left( 37 - \frac{\lambda}{3} - \frac{5\lambda^2}{144} \right) \quad (22)$$

and the displacement thickness is

$$\frac{\delta^*}{\Delta} = \int_0^1 (1 - w) d\eta^* = \frac{36 - \lambda}{120} \quad (23)$$

The general expression for the energy-loss thickness integral is obtained as

$$\begin{aligned} \frac{\varphi}{\Delta} &= \int_0^1 w(1 - \bar{t}) d\eta^* \\ &= \frac{7}{10} - \frac{13}{30} B_1 - \frac{13}{42} B_2 - \frac{67}{280} B_3 - \frac{7}{36} B_4 - \frac{103}{630} B_5 - \frac{31}{220} B_6 + \\ &\quad \frac{\lambda}{6} \left( \frac{1}{20} - \frac{1}{60} B_1 - \frac{1}{140} B_2 - \frac{1}{280} B_3 - \frac{1}{504} B_4 - \frac{1}{840} B_5 - \frac{1}{1320} B_6 \right) \quad (24) \end{aligned}$$

where  $B_2, B_3, \dots$  will be expressed in terms of  $B_1$  through the boundary conditions (eqs. (17), (20), and (21)). The corresponding expression for  $\Delta^*/\Delta$  is

$$\frac{\Delta^*}{\Delta} = \int_0^1 (1 - \bar{\tau}) d\eta^* = 1 - \frac{B_1}{2} - \frac{B_2}{3} - \frac{B_3}{4} - \frac{B_4}{5} - \frac{B_5}{6} - \frac{B_6}{7} \quad (25)$$

which will be used in the solution for the flow of a perfect gas.

The only integral in equations (9) and (10) as yet unspecified contains the density profile  $\rho_1/\rho$ . For the general case where equilibrium dissociation will be considered, the density ratio as determined from the data of reference 17 can be satisfactorily approximated by a fifth-degree polynomial in the enthalpy  $h$  and is

$$\frac{\rho_1}{\rho} = \frac{\rho_1}{\rho_B} \left[ b_1 + b_2 \frac{h}{h_B} + b_3 \left( \frac{h}{h_B} \right)^2 + b_4 \left( \frac{h}{h_B} \right)^3 + b_5 \left( \frac{h}{h_B} \right)^4 + b_6 \left( \frac{h}{h_B} \right)^5 \right] \quad (26)$$

In general, the quantities  $b_1, b_2, \dots$  will depend on the local pressure; however, as a first approximation these quantities are treated as constants. For a perfect gas and constant  $c_p$ , equation (26) reduces to

$$\frac{\rho_1}{\rho} = \frac{h}{h_1} = \frac{T}{T_1}$$

The enthalpy ratio  $h/h_B$  is expressed in terms of the stagnation-enthalpy-drop profile  $\bar{\tau}$  by the relation

$$\frac{h}{h_B} = \frac{c_{pW} T_W}{h_B} - \frac{u_1^2}{2h_B} w^2 + \left( \frac{h_1}{h_B} - \frac{c_{pW} T_W}{h_B} + \frac{u_1^2}{2h_B} \right) \bar{\tau}$$

from the definition of  $\bar{\tau}$ . For a perfect gas, this equation reduces to

$$\frac{h}{h_1} = \frac{T_W}{T_1} - \frac{u_1^2}{2h_1} w^2 + \left( 1 - \frac{T_W}{T_1} + \frac{u_1^2}{2h_1} \right) \bar{\tau}$$

The density integral  $\frac{\Omega}{\Delta} = \int_0^1 \left( \frac{\rho_1}{\rho} - \frac{u}{u_1} \right) d\eta^*$  can now be expressed in terms of  $\lambda$  and the stagnation enthalpy profile coefficients  $B_1, B_2, \dots$ . This integral is too lengthy to repeat here for the general case with dissociation; however, for a perfect gas, it becomes

$$\frac{\Omega}{\Delta} = \frac{\gamma - 1}{2} M_1^2 \frac{\theta}{\Delta} + \left( 1 + \frac{\gamma - 1}{2} M_1^2 \right) \left[ \frac{\delta^*}{\Delta} + \left( \frac{T_w}{T_1^*} - 1 \right) \frac{\Delta^*}{\Delta} \right] \quad (27)$$

The local skin-friction coefficient is by definition

$$c_f = \frac{\mu_w \left( \frac{\partial u}{\partial y} \right)_w}{\frac{1}{2} \rho_1 u_1^2}$$

or, when transformed to  $\eta^*$ ,

$$c_f = \frac{\mu_w}{\frac{1}{2} \rho_1 u_1} \frac{\rho_w}{\rho_1^*} \frac{1}{\Delta} \left( \frac{\partial w}{\partial \eta^*} \right)_w \quad (28)$$

Then, by using equations (15) and (12), the general relation is obtained

$$c_f \sqrt{\frac{\rho_w u_1 x}{\mu_w}} = 2 \sqrt{\frac{\rho_w}{\rho_1} \frac{x}{u_1} \frac{du_1}{dx} \frac{1}{\lambda} \frac{12 + \lambda}{6}} \quad (29)$$

which is dependent only on the wall temperature, the external flow, and the parameter  $\lambda$ .

Similarly, the local convective heat-transfer rate is defined as

$$q_w = -k_w \left( \frac{\partial T}{\partial y} \right)_w$$

or, when transformed to  $\eta^*$ ,

$$q_w = - \frac{k_w}{c_{p_w}} \frac{\rho_w}{\rho_1^*} t_1^* \left( \frac{\partial \bar{t}}{\partial \eta^*} \right)_w \frac{1}{\Delta} \quad (30)$$



since  $\left(\frac{\partial t^*}{\partial y}\right)_w = c_{p_w} \left(\frac{\partial T}{\partial y}\right)_w$ . Use of equations (15) and (16) in equation (30) then gives the relation

$$\frac{q_w x}{k_w T_w \sqrt{\frac{\rho_w x u_1}{\mu_w}}} = \left(1 - \frac{H_1}{c_{p_w} T_w}\right) \sqrt{\frac{\rho_1}{\rho_w} \frac{x}{u_1} \frac{du_1}{dx} \frac{1}{\lambda}} B_1 \quad (31)$$

which is dependent on the wall temperature, the external flow, and both  $\lambda$  and  $B_1$ .

#### APPLICATION TO FLOW OF A PERFECT GAS WITH CONSTANT $c_p$ AND $\sigma$

General equations.— When the results of the preceding section are used for a perfect gas together with the assumption that the thermal and velocity boundary layers are of equal thickness, equations (9) and (10) can be written as

$$\frac{d\theta}{dx} + \frac{1}{u_1} \frac{du_1}{dx} \left\{ \left(2 + \frac{\gamma - 1}{2} M_1^2\right) \theta + \left(1 + \frac{\gamma - 1}{2} M_1^2\right) \left[ \delta^* + \left(\frac{T_w}{T_1^*} - 1\right) \Delta^* \right] \right\} = \frac{\mu_w \rho_w}{u_1 (\rho_1^*)^2 \Delta} \frac{12 + \lambda}{6} \quad (32)$$

and

$$\frac{d\phi}{dx} + \phi \left( \frac{1}{u_1} \frac{du_1}{dx} - \frac{c_p}{t_1^*} \frac{dT_w}{dx} \right) = \frac{\mu_w \rho_w}{\sigma} \frac{B_1}{(\rho_1^*)^2 u_1 \Delta} \quad (33)$$

As an illustration of the detailed procedure, a fifth-degree temperature polynomial is used in the following development. This polynomial is chosen so as to satisfy two conditions at the edge of the boundary layer and two conditions at the wall. At the edge of the boundary layer, that is, at  $\eta^* = 1$ ,

$$\left. \begin{aligned} \bar{t} &= 1 \\ \frac{\partial \bar{t}}{\partial \eta^*} &= 0 \end{aligned} \right\} \quad (34)$$

These two conditions at  $\eta^* = 1$  give

$$B_4 = 5 - 4B_1 - 3B_2 - 2B_3$$

and

$$B_5 = -4 + 3B_1 + 2B_2 + B_3$$

Equations (24) and (25) may then be written as

$$\frac{\phi}{\Delta} = \alpha + \alpha_1 B_1 + \alpha_2 B_2 + \alpha_3 B_3 + \frac{\lambda}{6} (\alpha_4 + \alpha_5 B_1 + \alpha_6 B_2 + \alpha_7 B_3) \quad (35)$$

and

$$\frac{\Delta^*}{\Delta} = \frac{2}{3} - \frac{1}{5} B_1 - \frac{1}{15} B_2 - \frac{1}{60} B_3 \quad (36)$$

where the  $\alpha$ 's are constants and  $B_2$  and  $B_3$  depend on the known external flow, the parameter  $\lambda$ , and the wall temperature distribution as determined from the two wall conditions (eqs. (20) and (21)). Numerical values of the  $\alpha$  constants are given in table I. For a perfect gas and constant  $c_p$ , these wall conditions can be written as

$$B_2 = (1 - \sigma) \frac{\frac{\gamma - 1}{2} M_1^2 \left( \frac{12 + \lambda}{6} \right)^2}{T^*_{1}/T_1} \frac{1}{1 - \bar{T}_w} \quad (37)$$

and

$$B_3 = \frac{\sigma}{6} \frac{12 + \lambda}{6} \Delta^2 \frac{(\rho^*_{1})^2 u_1}{\rho_w T_w} \frac{1}{1 - \bar{T}_w} \frac{d\bar{T}_w}{dx} - (1 - \sigma) \frac{\frac{\gamma - 1}{2} M_1^2 \lambda \frac{12 + \lambda}{6}}{T^*_{1}/T_1} \frac{1}{1 - \bar{T}_w} \quad (38)$$

where  $\bar{T}_w = \frac{T_w}{T^*_{1}}$ .

Comparison with flat-plate flow:  $\frac{du_1}{dx} = 0$ . For  $\frac{du_1}{dx} = 0$ , the momentum equation (32) reduces to

$$\frac{d\theta}{dx} = 2 \frac{\mu_w \rho_w}{u_1 (\rho^*_1)^2 \Delta}$$

since  $\lambda = 0$ . By using equation (22) (with  $\lambda = 0$ ), this equation can be written as

$$\frac{37}{315} \frac{d\Delta}{dx} = \frac{2\mu_w \rho_w}{u_1 (\rho^*_1)^2 \Delta} \quad (39)$$

which by integration gives

$$\Delta^2 = 4 \frac{315}{37} \frac{1}{u_1 (\rho^*_1)^2} \int_0^x \mu_w \rho_w dx \quad (40)$$

Equations (37) and (38) can now be written as

$$B_2 = 4(1 - \sigma) \frac{\frac{\gamma - 1}{2} M_1^2}{\frac{T^*_1}{T_1} (1 - \bar{T}_w)} \quad (41)$$

and

$$B_3 = \frac{420}{37} \sigma \frac{d\bar{T}_w/dx}{1 - \bar{T}_w} \frac{1}{\rho_w \mu_w} \int_0^x \mu_w \rho_w dx \quad (42)$$

The energy equation (eq. (33)) is written for the flat plate as

$$\frac{d\phi}{dx} - \phi \frac{d\bar{T}_w/dx}{1 - \bar{T}_w} = \frac{\mu_w \rho_w}{\sigma u_1 (\rho^*_1)^2 \Delta} B_1 \quad (43)$$

or by using equation (35) with  $\lambda = 0$  and equations (41), (42), (39), and (40), equation (43) may be written as

$$\frac{dB_1}{dx} + B_1 \left[ \frac{1}{2f_w} \left( 1 - \frac{37}{630} \frac{1}{\sigma\alpha_1} \right) - \frac{d\bar{T}_w/dx}{1 - \bar{T}_w} \right] = - \frac{420}{37} \sigma \frac{\alpha_3}{\alpha_1} f_w \frac{d^2\bar{T}_w/dx^2}{1 - \bar{T}_w} +$$

$$\left[ \frac{\alpha}{\alpha_1} - \frac{210}{37} \sigma \frac{\alpha_3}{\alpha_1} \left( 1 + 2 \frac{df_w}{dx} \right) \right] \frac{d\bar{T}_w/dx}{1 - \bar{T}_w} - \frac{1}{2\alpha_1 f_w} \left[ \alpha + 4\alpha_2(1 - \sigma) \frac{\frac{\gamma - 1}{2} M_1^2}{T_{1}^*/T_1} \frac{1}{1 - \bar{T}_w} \right]$$

(44)

where  $f_w = \frac{1}{\mu_w \rho_w} \int_0^x \mu_w \rho_w dx$ . Integration of equation (44) gives the required solution for  $B_1$ .

In order to compare the results directly with those of reference 12 it is convenient to set  $f_w = x$ , whereupon the expression for  $B_1$  is

$$B_1 = \frac{1}{\alpha_1} \frac{(\bar{x})^{-m}}{\bar{T}_w - 1} \int \left\{ \frac{1}{\bar{x}} \left[ 2\alpha_2 \frac{(1 - \sigma) \frac{\gamma - 1}{2} M_1^2}{1 + \frac{\gamma - 1}{2} M_1^2} \frac{1}{\bar{T}_w - 1} - \frac{\alpha}{2} \right] + \right.$$

$$\left. \left( \frac{630}{37} \alpha_3 \sigma - \alpha \right) \frac{d\bar{T}_w/d\bar{x}}{\bar{T}_w - 1} + \frac{420}{37} \alpha_3 \sigma \bar{x} \frac{d^2\bar{T}_w/d\bar{x}^2}{\bar{T}_w - 1} \right\} (\bar{T}_w - 1) \bar{x}^m d\bar{x}$$

(45)

where  $\bar{x} = \frac{x}{L}$  and  $m = \frac{1}{2} - \frac{37}{1260\alpha_1\sigma}$ . From equations (30) and (40), the heat transfer is

$$q_w = - \frac{1}{2} \sqrt{\frac{37}{315}} k_1 T_1 C_w \left( 1 + \frac{\gamma - 1}{2} M_1^2 \right) (1 - \bar{T}_w) \sqrt{\frac{\rho_1 u_1}{\mu_1}} \frac{B_1}{\left( \int_0^x C_w dx \right)^{1/2}}$$

(46)

where  $C_w = \frac{k_w \rho_w}{k_1 \rho_1} = \frac{\mu_w \rho_w}{\mu_1 \rho_1}$  for a constant  $c_p$  and  $\sigma$ . The Chapman-Rubesin polynomial for the wall temperature distribution (ref. 12) is

$$\frac{T_w}{T_1} = \frac{T_e}{T_1} + \sum_{n=0}^{\infty} a_n \bar{x}^n \quad (47)$$

Substituting equation (45) (with  $T_w$  given by equation (47)) into equation (46) and integrating result in

$$q_w = \frac{1}{2} \sqrt{\frac{37}{315}} k_1 T_1 C_w \frac{\sqrt{\frac{\rho_1 u_1}{\mu_1}}}{\left(\int_0^x C_w dx\right)^{1/2}} \frac{1}{\alpha_1} \sum_{n=0}^{\infty} \left[ \alpha_3 \sigma \frac{420}{37} n^2 + \left( \alpha_3 \sigma \frac{210}{37} - \alpha \right) n - \frac{\alpha}{2} \frac{a_n \bar{x}^n}{n+m} \right] \quad (48)$$

Thus, in order to evaluate the accuracy of the heat transfer obtained from the present method by using a fifth-degree temperature profile, the expression

$$\frac{1}{\alpha_1} \sqrt{\frac{37}{315}} \left[ \alpha_3 \sigma \frac{420}{37} n^2 + \left( \alpha_3 \sigma \frac{210}{37} - \alpha \right) n - \frac{\alpha}{2} \right] \frac{1}{n+m} \quad (49)$$

is to be compared with the quantity  $-Y_n'(0)$  in the notation of reference 12. This comparison can be obtained from figure 1 where expression (49) is plotted against  $n$  for several different temperature profiles. (Numerical values of the  $\alpha$  constants are given in table I for several of the thermal profiles used.) The results are identified with the corresponding temperature profile by designating the degree of the polynomial and the number of wall and edge boundary conditions used to form the temperature profile. The quantity  $-Y_n'(0)$  from reference 12 is plotted in the same figure. Also shown in this figure is a table of

the percent error in the heat transfer as computed from the various thermal profiles for  $n = 0$  which corresponds to the case with  $\frac{dT_w}{dx} = 0$ .

Comparison of the results of the present method with the Chapman-Rubesin nonisothermal flat-plate solution shows that the sixth-degree (1 wall boundary condition, 4 edge boundary conditions), fifth-degree (2 wall, 2 edge), and sixth-degree (2 wall, 3 edge) stagnation temperature profiles may be expected to yield satisfactory heat-transfer computations when the wall temperature distribution can be approximated by a polynomial in which the lower order terms ( $n < 5$ ) predominate. However, it is important to note that a polynomial for the wall temperature is not required in the present method. Thus, a general conclusion applicable here is that the heat-transfer values would be in some error towards the rear of the body ( $\bar{x} > \frac{1}{2}$ ) if the temperature distribution in this region is characterized by large gradients. The reason for the error in the present method under this condition is probably the assumption of equal thermal and velocity boundary-layer thicknesses since the exact solution of reference 20 shows that the thickness of the thermal layer is reduced by increasing  $n$ .

For the purpose of comparison with the exact solution, the equilibrium temperature  $T_e$  for the flat plate can be obtained from equation (45) with  $B_1 = 0$  (corresponding to  $q_w = 0$ ) and  $T_w = T_e = \text{Constant}$ . Thus,

$$2\alpha_2 \frac{(1 - \sigma) \frac{\gamma - 1}{2} M_1^2}{1 + \frac{\gamma - 1}{2} M_1^2} - \frac{\alpha_2}{2\alpha} \left( \frac{T_e}{T_1^*} - 1 \right) = 0$$

or

$$\frac{T_e}{T_1} = 1 + \frac{\gamma - 1}{2} M_1^2 + 4 \frac{\alpha_2}{\alpha} (1 - \sigma) \frac{\gamma - 1}{2} M_1^2$$

from which the recovery factor is

$$F_r = 1 + 4 \frac{\alpha_2}{\alpha} (1 - \sigma)$$

The values of  $F_r$  for six different temperature profiles are plotted against  $\sigma$  in figure 2. These values are to be compared with the recovery factor from the exact solution (taken as  $F_r = \sqrt{\sigma}$ ) which is also plotted in figure 2.

The recovery factors resulting from the use of the fifth-degree thermal profile (with 2 wall and 2 edge boundary conditions) are evidently accurate to within a few percent over the range of Prandtl numbers applicable to gases. Note that for the same number of wall boundary conditions the recovery factor approaches unity as the number of stream conditions is increased. This somewhat anomalous result can probably be attributed to the effect of the assumption of equal velocity and thermal boundary-layer thicknesses.

The wall shear stress

$$\tau_w = \mu_w \left( \frac{\partial u}{\partial y} \right)_w$$

is independent of the temperature profile and can be written as

$$\tau_w = \sqrt{\frac{37}{315}} u_1 C_w \sqrt{\frac{u_1 \mu_1 \rho_1}{\int_0^x C_w dx}} \quad (50)$$

by transforming to  $\eta^*$  and using equation (40) for  $\Delta$  and equations (12) for  $\left( \frac{\partial w}{\partial \eta^*} \right)_w$  with  $\lambda = 0$ .

Note that equation (50) can be put into the same form as the corresponding result in reference 12 by setting  $C_w = C$  under the integral only, where  $C$  is a constant equal to the average value of  $C_w$ . This constant  $C$  was used in a similar manner in the solution of reference 12; hence, equation (50) differs from the exact solution only in the value of the numerical factor  $\sqrt{37/315}$  which is about 3 percent too high.

Comparison with stagnation flow:  $u_1$  approaches 0.- Approximate expressions for the heat transfer in the stagnation region of a blunt-nose body can be derived by noting that, in order to avoid infinite values of  $d\theta/dx$  and  $d\phi/dx$  as  $u_1$  approaches 0 in equations (32) and (33), the following equations must be satisfied:

$$\left[ 2\theta + \delta^* + (\bar{T}_w - 1)\Delta^* \right] \frac{du_1}{dx} - \frac{\mu_w \rho_w}{(\rho^*_1)^2 \Delta} \frac{12 + \lambda}{6} = 0$$

and

$$\varphi \frac{du_1}{dx} - \frac{\mu_w \rho_w}{\sigma (\rho^*_1)^2 \Delta} B_1 = 0$$

By using equation (15), these conditions can be written as

$$2 \frac{\theta}{\Delta} + \frac{\delta^*}{\Delta} + (\bar{T}_w - 1) \frac{\Delta^*}{\Delta} - \bar{T}_w \frac{12 + \lambda}{6\lambda} = 0 \quad (51)$$

and

$$\frac{\varphi}{\Delta} - \bar{T}_w \frac{B_1}{\sigma \lambda} = 0 \quad (52)$$

where for this case  $\frac{\rho_1}{\rho_w} = \frac{T_w}{T_1} = \frac{T_w}{T^*_1} = \bar{T}_w$ . For  $u_1 = 0$ , the quantities  $B_2$  and  $B_3$  are both zero so that from equations (35) and (36)

$$\frac{\varphi}{\Delta} = \alpha + \alpha_1 B_1 + \frac{\lambda}{6} (\alpha_4 + \alpha_5 B_1) \quad (53)$$

and

$$\frac{\Delta^*}{\Delta} = \frac{2}{3} - \frac{1}{5} B_1 \quad (54)$$

Note that the constants given in equation (54) apply only for the particular fifth-degree temperature profile used in this section. For any other profile, the constants can be easily obtained from equation (25) and the desired boundary conditions. Using equations (53) and (54) and eliminating  $B_1$  between equations (51) and (52) give the following relation between  $\bar{T}_w$  and  $\lambda$ :



$$\begin{aligned} & \bar{T}_w^2 \left( \frac{2}{3} - \frac{12 + \lambda}{6\lambda} \right) + \bar{T}_w \left[ 2 \frac{\theta}{\Delta} + \frac{\delta^*}{\Delta} - \frac{2}{3} - \sigma \left( \alpha_1 + \frac{\lambda}{6} \alpha_5 \right) \left( \frac{2}{3} \lambda - \frac{12 + \lambda}{6} \right) - \right. \\ & \left. \frac{1}{5} \sigma \lambda \left( \alpha + \frac{\lambda}{6} \alpha_4 \right) \right] - \sigma \lambda \left( \alpha_1 + \frac{\lambda}{6} \alpha_5 \right) \left( 2 \frac{\theta}{\Delta} + \frac{\delta^*}{\Delta} - \frac{2}{3} \right) + \frac{1}{5} \sigma \lambda \left( \alpha + \frac{\lambda}{6} \alpha_4 \right) = 0 \end{aligned} \quad (55)$$

(Eqs. (22) and (23) are used for  $\frac{\theta}{\Delta}$  and  $\frac{\delta^*}{\Delta}$ .)

Defining a Nusselt number for stagnation flow as

$$\text{Nu} = \frac{q_w L}{k_1 (T_w - T_1^*)}$$

and using equation (31) gives

$$\frac{\text{Nu}}{\sqrt{\frac{\rho_1 L}{\mu_1} \frac{du_1}{d\bar{x}}}} = \sqrt{\frac{\mu_w}{\mu_1} \frac{B_1}{\lambda}} \quad (56)$$

for constant  $c_p$  and  $\sigma$ . This expression is plotted against  $T_w/T_1$  in figure 3 for five temperature profiles. The corresponding values from the exact solutions of references 13 and 14 are plotted in figure 3 for comparison. Apparently, the present method can be expected to give accurate results for this type of flow only for  $\frac{T_w}{T_1} < 0.7$  and when the fourth- or fifth-degree temperature profiles are used with two edge conditions. Consideration of the shape of the temperature and velocity profiles given in reference 13 indicates that the erroneous results of the present method for heating conditions  $\left( \frac{T_w}{T_1} > 1 \right)$  are probably due to the inherent limitations of the velocity profile rather than to the assumption of equal thermal and velocity boundary-layer thicknesses.

Comparison with experimental recovery factors:  $q_w = 0$ . - The recovery factors on a flat plate were calculated with good accuracy by using the fifth-degree stagnation-temperature profile with two edge and two wall boundary conditions. (See fig. 2.) Therefore, as a further check on the range of applicability of the present method,

this particular profile only is used to compute the recovery factors on a circular cylinder for comparison with the data of Eber (ref. 16).

For zero heat transfer,  $q_w = 0$ ; hence, from equation (31)  $B_1 = 0$  and the integral momentum and energy equations (eqs. (32) and (33)) may then be written as

$$\frac{dz}{d\bar{x}} + 2z \left\{ 2 + \frac{\gamma - 1}{2} M_1^2 + \left( 1 + \frac{\gamma - 1}{2} M_1^2 \right) \left[ \frac{\delta^*}{\theta} + (t_e - 1) \frac{\Delta^*}{\theta} \right] \right\} \frac{1}{u_1} \frac{du_1}{d\bar{x}} = 2C_w \frac{R_{OL} \left( \frac{\rho_1}{\rho^*_1} \right)^2}{R_{1L} \left( \rho^*_1 \right)^2} \frac{\theta}{\Delta} \frac{12 + \lambda}{6} \quad (57)$$

and

$$\frac{d\bar{\varphi}}{d\bar{x}} + \bar{\varphi} \left( \frac{1}{u_1} \frac{du_1}{d\bar{x}} + \frac{1}{t_e - 1} \frac{dt_e}{d\bar{x}} \right) = 0 \quad (58)$$

where

$$\frac{T_w}{T^*_1} = \frac{T_e}{T^*_1} = t_e$$

and

$$z = R_{OL} \left( \frac{\theta}{\Delta} \right)^2 \left( \frac{\Delta}{L} \right)^2 = \frac{R_{OL}}{R_{1L}} C_w \lambda \left( \frac{\theta}{\Delta} \right)^2 \frac{\left( \frac{\rho_1}{\rho^*_1} \right)^2 \frac{T_1}{T^*_1}}{t_e \frac{1}{u_1} \frac{du_1}{d\bar{x}}} \quad (59)$$

The quantity  $Z$  has been introduced to avoid the use of  $d^2u_1/dx^2$  as is done in the Holstein-Bohlen method. Equation (15) was used for  $\Delta^2$  in equation (59).

A relation between  $\lambda$  and  $t_e$  can be obtained by integration of equation (58) which gives

$$\frac{\Phi}{\Delta L} u_1(t_e - 1) = \text{Constant} = 0 \quad (60)$$

since, at  $x = 0$ ,  $u_1 = 0$  for a body with a blunt leading edge and  $\frac{\Phi}{L} = 0$  for a body with a sharp leading edge. By using equations (35), (37), (38), and (15), equation (60) can be written

$$\frac{\sigma}{6} \frac{\lambda \frac{12 + \lambda}{6} \frac{dt_e}{d\bar{x}}}{\frac{T_1^*}{T_1} \frac{1}{u_1} \frac{du_1}{d\bar{x}}} - \frac{\alpha + \frac{\lambda}{6} \alpha_4}{\alpha_3 + \frac{\lambda}{6} \alpha_7} t_e^2 + t_e \left[ \frac{\alpha + \frac{\lambda}{6} \alpha_4}{\alpha_3 + \frac{\lambda}{6} \alpha_7} + \right. \\ \left. (1 - \sigma) \frac{\frac{\gamma - 1}{2} M_1^2}{1 + \frac{\gamma - 1}{2} M_1^2} \frac{12 + \lambda}{6} \left( \frac{\alpha_2 + \frac{\lambda}{6} \alpha_6}{\alpha_3 + \frac{\lambda}{6} \alpha_7} \frac{12 + \lambda}{6} - \lambda \right) \right] = 0 \quad (61)$$

which can be integrated by substituting a new dependent variable for  $t_e^{-1}$ . Thus, equations (57), (59), and (61) are to be solved simultaneously for  $Z$ ,  $\lambda$ , and  $t_e$ .

In the terminology of reference 21, the "local" recovery factor is defined as

$$F_r = \frac{t_e - \frac{T_1}{T_1^*}}{1 - \frac{T_1}{T_1^*}} \quad (62)$$

whereas a "local free stream" recovery factor is defined as

$$F_{r'} = \frac{t_e - \frac{T_\infty}{T_\infty^*}}{1 - \frac{T_\infty}{T_\infty^*}} \quad (63)$$

where in general  $T_1^* = T_\infty^*$ . Both of these recovery factors have been calculated by the present method for a circular cylinder with axis normal to the flow. The values of  $u_1$  and  $du_1/dx$  needed in the calculation were determined from unpublished data obtained in the Gas Dynamics Branch of the Langley Laboratory. These data were run at a free-stream Mach number of 1.98 and free-stream Reynolds number based on cylinder diameter of  $1.2 \times 10^6$ . The resulting pressure distribution could be closely approximated by the empirical relation

$$\frac{p_1}{p_\infty} = \frac{\gamma}{2} M_\infty^2 (0.67 + 0.98 \cos 3.27\bar{x}) + 1 \quad (64)$$

for  $0 \leq \frac{x}{L} < 0.96$ . (The symbol  $L$  denotes the diameter.)

The general procedure used in the calculation was as follows: As a first approximation, it was assumed that  $t_e = 1$ ; equations (57) and (59) were then solved simultaneously for  $Z$  and  $\lambda$  by the method of isoclines. By using these values of  $\lambda$ , a second approximation to the values of  $t_e$  against  $x$  was obtained from equation (61). With the new values of  $t_e$ , the process can then be repeated to convergence. Actually, in the example given, the second approximation for  $t_e$  was sufficiently accurate since the use of this second approximation produced no significant change in the values of  $\lambda$  against  $x$  determined from equations (57) and (59).

The recovery factors  $F_r$  and  $F_{r'}$  resulting from this calculation have been plotted in figure 4. The values of  $F_{r'}$  from the data of Eber (ref. 16) and  $F_r$  from the data of Eckert and Weise (ref. 22) are plotted in the same figure. Apparently, the conclusion already obtained by several investigators for subsonic flow (for example, ref. 22 with general discussions available in refs. 21 and 23) that  $F_r \approx \sqrt{\sigma}$ , regardless of body shape or axial station, is substantiated by the present results for supersonic flow about a cylinder. This result is also known to be valid for a pointed body of revolution as shown in reference 24.

Comparison with exact solution for heat transfer on a cylinder:

$\sigma = 1$ ;  $M_1 \approx 0$ ;  $\frac{T_w}{T_1} \approx 1$ . - An exact solution for the heat transfer on a cylinder was given by Goland (ref. 15). The solution postulates constant gas properties and hence would be strictly applicable only to incompressible flow with  $T_w/T_1$  in the neighborhood of unity. As already shown by comparison with exact values (fig. 3), the best results of the present method are in error by about 10 percent at  $\frac{T_w}{T_1} \approx 1$  for stagnation flow. Nevertheless, a comparison of this method with Goland's exact solution would be useful as an indication of the accuracy of the present method with an arbitrary pressure gradient.

For calculation of the heat transfer under the most general conditions, that is, in compressible flow with arbitrary pressure and wall temperature gradients and arbitrary Prandtl number near unity, it is convenient to write equations (32) and (33) in the following form:

$$\frac{dZ}{d\bar{x}} + 2Z \left\{ 2 + \frac{\gamma - 1}{2} M_1^2 + \left( 1 + \frac{\gamma - 1}{2} M_1^2 \right) \left[ \frac{\delta^*}{\theta} + (\bar{T}_w - 1) \frac{\Delta^*}{\theta} \right] \right\} \frac{1}{u_1} \frac{du_1}{d\bar{x}} =$$

$$2C_w \frac{R_{OL}}{R_{1L}} \left( \frac{\rho_1}{\rho^*_1} \right)^2 \frac{\theta}{\Delta} \frac{12 + \lambda}{6} \quad (65)$$

and

$$\frac{d\bar{\theta}}{d\bar{x}} + \frac{\bar{\theta}}{\bar{H}} \frac{d\bar{H}}{d\bar{x}} + \bar{\theta} \left( \frac{1}{u_1} \frac{du_1}{d\bar{x}} + \frac{d\bar{T}_w/d\bar{x}}{\bar{T}_w - 1} \right) = \frac{C_w}{\sigma R_{1L}} \left( \frac{\rho_1}{\rho^*_1} \right)^2 \frac{L}{\Delta} \frac{B_1}{\bar{H}} \quad (66)$$

where

$$Z = \frac{R_{OL}}{R_{1L}} C_w \lambda \left( \frac{\theta}{\Delta} \right)^2 \frac{\left( \frac{\rho_1}{\rho^*_1} \right)^2 \frac{T_1}{T^*_1}}{\bar{T}_w \frac{1}{u_1} \frac{du_1}{d\bar{x}}} \quad (67)$$

and

$$\bar{H} = \frac{\Phi}{\theta} \quad (68)$$

Equations (65) and (67) are of the same form as equations (57) and (59) in the preceding section except that  $t_e$  has been replaced by  $\bar{T}_w$  and  $B_1 \neq 0$ . Subtraction of the momentum equation (32) from equation (66) and use of equation (15) for  $\Delta/L$  results in

$$\frac{d}{d\bar{x}} \log \bar{H} - \left[ 1 + \frac{\delta^*}{\theta} + \frac{\Delta^*}{\theta} (\bar{T}_w - 1) \right] \frac{1}{M_1} \frac{dM_1}{d\bar{x}} + \frac{\frac{d\bar{T}_w}{d\bar{x}}}{\bar{T}_w - 1} = \frac{\bar{T}_w}{\lambda} \frac{1}{u_1} \frac{du_1}{d\bar{x}} \left( \frac{B_1}{\sigma \bar{H}} - \frac{12 + \lambda}{6} \right) \quad (69)$$

which is more suitable for use in the general computational procedure than equation (66). The one-dimensional adiabatic energy equation

$$\frac{du_1}{u_1} = \frac{1}{1 + \frac{\gamma - 1}{2} M_1^2} \frac{dM_1}{M_1}$$

has been used in equation (69) for the flow outside the boundary layer. Thus, equations (65), (67), (68), and (69) are to be solved simultaneously for  $Z$ ,  $\lambda$ ,  $\bar{H}$ , and  $B_1$  by a suitable modification of the method of isoclines. The quantities  $\frac{\delta^*}{\Delta}$ ,  $\frac{\theta}{\Delta}$ ,  $\frac{\Delta^*}{\Delta}$ , and  $\frac{\Phi}{\Delta}$  are all functions of  $\lambda$  and  $B_1$  as outlined previously.

For application to the problem considered herein, equations (65), (69), (67), and (68) reduce to the form

$$\frac{dZ}{d\bar{x}} + 2Z \left[ 2 + \frac{\delta^*}{\theta} + (\bar{T}_w - 1) \frac{10 - 3B_1}{15 \frac{\theta}{\Delta}} \right] \frac{1}{u_1} \frac{du_1}{d\bar{x}} = 2C_w \frac{R_{oL}}{R_{1L}} \frac{\theta}{\Delta} \frac{12 + \lambda}{6} \quad (70)$$

$$\frac{d}{d\bar{x}} \log \bar{H} - \left[ 1 + \frac{\delta^*}{\theta} + (\bar{T}_w - 1) \frac{10 - 3B_1}{15 \frac{\theta}{\Delta}} \right] \frac{1}{u_1} \frac{du_1}{d\bar{x}} = \frac{\bar{T}_w \frac{1}{u_1} \frac{du_1}{d\bar{x}}}{\lambda \frac{\theta}{\Delta}} \left( \frac{B_1}{\bar{H}} - \frac{12 + \lambda}{6} \right) \quad (71)$$

$$z = \frac{R_{oL}}{R_{1L}} C_w \lambda \left( \frac{\theta}{\Delta} \right)^2 \frac{u_1}{\bar{T}_w \frac{du_1}{d\bar{x}}} \quad (72)$$

and

$$\bar{H} = \frac{\varphi}{\theta} = \frac{a + a_1 B_1 + \frac{\lambda}{6} (a_4 + a_5 B_1)}{\frac{1}{315} \left( 37 - \frac{\lambda}{3} - \frac{5\lambda^2}{144} \right)} \quad (73)$$

for  $B_2 = B_3 = 0$ , since  $M_1 = 0$ ,  $\sigma = 1$ , and  $T_w$  is a constant. Note that the gas properties are not necessarily constant.

The same expression for the Nusselt number as given by equation (56) can be used in this problem since  $T^*_1 = T_1 = T_e = T_\infty$  for low-speed flow. Thus, from equation (56)

$$\frac{Nu}{\sqrt{R_{\infty L}}} = \frac{q_w L}{k_\infty (T_w - T_\infty)} \sqrt{\frac{\mu_\infty}{\rho_\infty u_\infty L}} = \sqrt{\frac{\mu_w}{\mu_\infty}} \sqrt{\frac{1}{\lambda u_\infty} \frac{du_1}{d\bar{x}}} B_1 \quad (74)$$

Inasmuch as the present method is expected to supply accurate heat-transfer values only under cooling conditions, the calculation has been carried out for  $\frac{T_w}{T_1} = 0.74$ . This value gives starting values of  $\lambda = 6.00$  and  $B_1 = 1.516$  from equations (55) and (52). The results in the form of  $Nu/\sqrt{R_{\infty L}}$  are shown in figure 5 together with the corresponding values

given by Goland. Over the forward portion of the body the heat-transfer coefficients from the present method differ from the exact values by about 5 percent; however, at least half of this difference is due to the effect of variable gas properties as shown by comparison of Squire's solution (ref. 14) with the results of reference 13. The assumption of equal thermal and velocity boundary-layer thicknesses apparently gives good results in this case.

The computation procedure for this particular problem was fairly simple since the energy and momentum equations were found to be practically independent. (For  $\frac{T_w}{T_1} = 1$  these equations would be entirely independent.) Thus, as a first approximation,  $B_1$  was considered constant and equations (70) and (72) were then used to compute  $Z$  and  $\lambda$  against  $\bar{x}$ . With this curve of  $\lambda$  against  $\bar{x}$ , the quantities  $\bar{H}$  and  $B_1$  were computed from equations (71) and (73). This second approximation for the  $B_1$  curve was then used to recompute  $Z$  and  $\lambda$  from equations (70) and (72); however, if allowance is made for computational error, the new values of  $\lambda$  are the same as the first values.

#### APPLICATION TO FLOW WITH EQUILIBRIUM DISSOCIATION

In a recent paper by Moore (ref. 17) the laminar boundary-layer characteristics with equilibrium dissociation were computed for a flat plate. One of the conclusions obtained was that the heat-transfer rate per unit area is essentially unaffected by dissociation when the plate temperature is below 2,500° R. If an analogous conclusion could be obtained for the flow in the stagnation region of a blunt-nose body, the equilibrium dissociation would clearly be expected to have little effect on the heat transfer at any point (in the laminar flow) on an arbitrary body. Presumably, a heat-transfer calculation could be carried out on any body with known velocity and wall temperature distributions by the present method (as indicated in the section entitled "General Method of Solution"). In view of the above statement, however, it is desirable to compute the heat transfer for the stagnation flow first.

According to results previously given (fig. 3) for the heat transfer in the stagnation region with a perfect gas flow, there is little choice between the fourth- and fifth-degree temperature profiles for this purpose. Hence, for computational simplicity, a fourth-degree enthalpy profile with two edge and one wall boundary condition is used in this section. Thus, using equation (26) to express the density ratio  $\rho_1/\rho$  as a function of enthalpy and taking the limiting conditions from



equations (9) and (10) for  $u_1$  approaching 0 (as indicated previously for a perfect gas) result in the following two simultaneous equations for  $\lambda$  and  $B_1$ :

$$K_0 + K_1 B_1 + K_2 B_1^2 + K_3 B_1^3 + K_4 B_1^4 + K_5 B_1^5 = \frac{\rho_B}{\rho_1} \left( \frac{7}{10} + \frac{\lambda}{120} \right) + \frac{\rho_B}{\rho_w} \frac{12 + \lambda}{6\lambda} - \frac{\rho_B}{\rho_1} \frac{2}{315} \left( 37 - \frac{\lambda}{3} - \frac{5\lambda^2}{144} \right) \quad (75)$$

and

$$B_1 = \frac{\sigma_w \lambda \left( \alpha + \frac{\lambda}{6} \alpha_3 \right)}{\frac{\rho_1}{\rho_w} - \sigma_w \lambda \left( \alpha_1 + \frac{\lambda}{6} \alpha_4 \right)} \quad (76)$$

The  $K$ 's are constants depending on the values of the stream enthalpy  $h_1$ , the wall temperature  $T_w$ , and the  $b$ 's in equation (26).

Defining a wall Nusselt number in terms of the wall values and stream enthalpy as

$$Nu_w = \frac{q_w L}{k_w \left( T_w - \frac{h_1}{c_{p_w}} \right)}$$

and using equation (31) for the heat transfer give a heat-transfer parameter of the form

$$\frac{Nu_w}{\sqrt{\frac{\rho_w L}{\mu_w} \frac{du_1}{d\bar{x}}}} = B_1 \sqrt{\frac{\rho_1 / \rho_w}{\lambda}}$$

which is directly proportional to the heat-transfer rate for constant  $T_w$  and  $h_1$ . This parameter is plotted in figure 6 against  $h_1/h_B$  for  $T_w = 2,000^\circ \text{R}$ . The heat-transfer values for a perfect gas with no dissociation are also plotted in figure 6 together with the corresponding density changes.

According to these results, the equilibrium dissociation has a negligible effect on the heat-transfer rate at a stagnation point. This conclusion is, of course, to be regarded with caution owing to the inherent limitations of the method. Thus, for example, the velocity and enthalpy profile shapes are controlled only by stream and wall conditions. This limitation indicates that application of the present method to the flat plate would result in no effect of dissociation as long as the stream and wall temperatures are below dissociation values. Since this result agrees qualitatively with the results of Moore (ref. 17), the over-all profile shapes are apparently not too important if the wall and stream values can be given accurately.

Another disadvantage of the present method for application to dissociation flow is associated with the assumption of equal thermal and velocity boundary-layer thicknesses. The dissociation data of reference 17 show that the Prandtl number increases to a maximum of 5 or 6 for increasing dissociation. This increase would normally imply a smaller thermal boundary-layer thickness in comparison to the velocity thickness. However, as noted previously, the computations of reference 20 indicate that the thermal layer would be about 70 percent of the velocity layer even for an increase in Prandtl number to 5 throughout the entire boundary layer. Probably then, the present results are fairly reliable.

### CONCLUSIONS

The application of the Von Kármán-Pohlhausen integral method to the laminar boundary layer of a flowing gas has been simplified for the general case of arbitrary stream velocity and wall temperature distributions. The principal simplifying assumptions and procedures are (1) equal thermal and velocity boundary-layer thicknesses, (2) linear viscosity-temperature relation, (3) use of the first coefficient in the polynomial for the stagnation temperature profile as one of the unknowns in the final solution of the momentum and energy equations, and (4) application of the Holstein-Bohlen method to avoid the use of the second derivative of the stream velocity.

Comparison of the results of the present method with the Chapman-Rubesin nonisothermal flat-plate solution (Jour. Aero. Sci., Sept. 1949) shows that the sixth-degree (1 wall boundary condition, 4 edge boundary

conditions), fifth-degree (2 wall boundary conditions, 2 edge boundary conditions), and sixth-degree (2 wall boundary conditions 3 edge boundary conditions) stagnation-temperature profiles may be expected to yield accurate heat-transfer computations except when the wall temperature distributions are characterized by large gradients toward the rear of the body, a condition which would seldom be realized in flight. The reason for the errors in the present method under this condition is probably the assumption of equal thermal and velocity boundary-layer thicknesses since the exact solution of Levy (Jour. Aero. Sci., May 1952) shows that the thickness of the thermal boundary layer is reduced by increasing the wall temperature gradient.

On the other hand, the heat transfer in the stagnation region of a blunt-nose body is given accurately only by the fourth-degree (1 wall boundary condition, 2 edge boundary conditions) and the fifth-degree (2 wall boundary conditions, 2 edge boundary conditions) thermal profiles when the wall temperature is less than the local equilibrium temperature. The error of the present method in this case, however, appears to be caused by the inherent limitations on the velocity profile (as shown by comparison with the results of Brown and Donoughe in NACA TN 2479) rather than the assumption of equal thermal and velocity boundary-layer thicknesses.

The recovery factors on both the flat plate and circular cylinder in supersonic flow were computed satisfactorily with the fifth-degree (2 wall boundary conditions, 2 edge boundary conditions) profile. The local recovery factors on the cylinder were independent of location and nearly equal to the square root of the Prandtl number. These results are in agreement with those already obtained by several investigators for subsonic flow.

The above results tend to indicate that the fifth-degree stagnation temperature or enthalpy profile will probably give the best over-all accuracy for the heat-transfer calculations by the present method on an arbitrary body for the case of heat transfer from the flowing gas to the surface. This conclusion is substantiated by comparison of the results obtained from the use of the fifth-degree profile with the exact solution of Goland (Jour. Aero. Sci., July 1950) for the heat transfer on a cylinder.

As an illustration of possible applications of the method, the heat transfer was calculated in the stagnation region of a blunt body with equilibrium dissociation. According to this calculation the equilibrium dissociation has a negligible effect on the heat-transfer rate at a stagnation point. However, the results obtained for this

extreme case should be taken as indicative only of order of magnitude because of the inherent limitations of the method.

Langley Aeronautical Laboratory,  
National Advisory Committee for Aeronautics,  
Langley Field, Va., June 19, 1953.

## APPENDIX

THE EFFECT OF LATERAL RADIUS OF CURVATURE ON SKIN FRICTION  
AND HEAT TRANSFER IN THE LAMINAR BOUNDARY LAYER

Seban and Bond (ref. 25) have given a solution by power series of the incompressible-laminar-boundary-layer equations for a slender circular cylinder with axis parallel to the flow. The conclusion was obtained that the changes in heat transfer and skin friction due to the effect of lateral radius of curvature are negligible until the square root of the body Reynolds number is of the order of or less than 100 times the body fineness ratio.

The results of this solution substantially confirm the earlier results of an approximate solution by Young (ref. 26) in regard to the changes in skin friction. Young used the Von Kármán-Pohlhausen integral method but assumed the velocity-profile shape to be invariant over the entire body length. Although the effects of lateral radius of curvature are certainly negligible for practical body configurations at subsonic speeds, these effects may become appreciable at supersonic speeds because of the large relative increases in wall temperature.

The purpose of this appendix is to show how the application of the Von Kármán-Pohlhausen method to this problem may be simplified for compressible flow by means of a modified Dorodnitsyn transformation. The pressure gradient is assumed negligible since the results are likely to be of importance only for bodies of high fineness ratio. However, in accordance with the physical requirements (even for zero pressure gradient) the dimensionless temperature and velocity-profile shapes are allowed to change along the body length.

The boundary-layer equations for the case of zero axial-pressure gradient and constant  $c_p$  and  $\sigma$  are written as follows:

Momentum:

$$\rho u r \frac{\partial u}{\partial x} + \rho v r \frac{\partial u}{\partial y} = \frac{\partial}{\partial y} \left( r \mu \frac{\partial u}{\partial y} \right) \quad (A1)$$

$$0 = \frac{\partial p}{\partial y}$$

Continuity:

$$\frac{\partial}{\partial x}(\rho ur) + \frac{\partial}{\partial y}(\rho vr) = 0 \quad (A2)$$

Energy:

$$\rho ur c_p \frac{\partial T}{\partial x} + \rho v r c_p \frac{\partial T}{\partial y} = \frac{\partial}{\partial y} \left( r k \frac{\partial T}{\partial y} \right) + r \mu \left( \frac{\partial u}{\partial y} \right)^2 \quad (A3)$$

In terms of the stagnation temperature defined as

$$T^* = T + \frac{u^2}{2c_p}$$

equation (A3) may be written

$$\rho ur \frac{\partial T^*}{\partial x} + \rho vr \frac{\partial T^*}{\partial y} = \frac{\partial}{\partial y} \left( r \mu \frac{\partial T^*}{\partial y} \right) + \left( \frac{1}{\sigma} - 1 \right) \frac{\partial}{\partial y} \left( r \mu \frac{\partial T}{\partial y} \right) \quad (A4)$$

Integrating equations (A1) and (A4) across the boundary layer and using equation (A2) gives

$$\frac{d}{dx} \int_0^\infty \left( \frac{u}{u_1} - \frac{u^2}{u_1^2} \right) \frac{\rho}{\rho^*_{1}} \frac{r}{L} dy = \frac{r_w t_w}{\rho^*_{1} u_1 L} \left( \frac{\partial w}{\partial y} \right)_w \quad (A5)$$

and

$$\frac{d}{dx} \int_0^\infty \frac{u}{u_1} \left( 1 - \frac{t^*}{t^*_{1}} \right) \frac{\rho}{\rho^*_{1}} \frac{r}{L} dy - \frac{1}{t^*_{1}} \frac{dT_w}{dx} \int_0^\infty \frac{u}{u_1} \left( 1 - \frac{t^*}{t^*_{1}} \right) \frac{\rho}{\rho^*_{1}} \frac{r}{L} dy = \frac{r_w t_w}{\sigma \rho^*_{1} u_1 L} \left( \frac{\partial t}{\partial y} \right)_w \quad (A6)$$

If a modified Dorodnitsyn transformation of the form

$$\eta_r = \int_0^y \frac{\rho}{\rho_1^*} \frac{r}{L} dy \quad (A7)$$

is introduced, equations (A5) and (A6) can be written as

$$\frac{d}{dx} \int_0^\infty \left( \frac{u}{u_1} - \frac{u^2}{u_1^2} \right) d\eta_r = \frac{\mu_w \rho_w}{(\rho_1^*)^2 u_1} \left( \frac{r_w}{L} \right)^2 \left( \frac{\partial w}{\partial \eta_r} \right)_w \quad (A8)$$

and

$$\frac{d}{dx} \int_0^\infty \frac{u}{u_1} \left( 1 - \frac{t^*}{t_1^*} \right) d\eta_r - \frac{1}{t_1^*} \frac{dT_w}{dx} \int_0^\infty \frac{u}{u_1} \left( 1 - \frac{t^*}{t_1^*} \right) d\eta_r = \frac{\mu_w \rho_w}{\sigma (\rho_1^*)^2 u_1} \left( \frac{r_w}{L} \right)^2 \left( \frac{\partial \bar{t}}{\partial \eta_r} \right)_w \quad (A9)$$

The wall boundary conditions for the velocity and stagnation-temperature profiles are derived from equations (A1) and (A4) evaluated at  $y = 0$ . When the viscosity and density relations given by equations (13) and (14) and the transformation from equation (A7) are used, these wall conditions may be written as

$$\left( \frac{\partial^2 w}{\partial \eta_r^2} \right)_w + \frac{2}{L} \frac{\cos \beta_w}{\frac{\rho_w}{\rho_1^*} \left( \frac{r_w}{L} \right)^2} \left( \frac{\partial w}{\partial \eta_r} \right)_w = 0 \quad (A10)$$

and

$$\left( \frac{\partial^2 \bar{t}}{\partial \eta_r^2} \right)_w + \frac{2}{L} \frac{\cos \beta_w}{\frac{\rho_w}{\rho_1^*} \left( \frac{r_w}{L} \right)^2} \left( \frac{\partial \bar{t}}{\partial \eta_r} \right)_w = (1 - \sigma) \frac{u_1^2}{c_p t_1^*} \left( \frac{\partial w}{\partial \eta_r} \right)_w^2 \quad (A11)$$

Note that, for  $\sigma = 1$ , these equations would be of the same form and, consequently, the velocity-profile shape  $w$  against  $\eta/\delta$  and the stagnation-temperature-profile shape  $\bar{t}$  against  $\eta/\Delta$  would both be exactly the same if the same number of edge boundary conditions were used in both profiles. Furthermore, if  $\delta = \Delta$  (with  $\sigma = 1$ ), equation (A9) must reduce to the same form as equation (A8), so that under these conditions the additional equality  $\frac{dT_w}{dx} = 0$  is required. The effect of the wall temperature gradient for a body of high fineness ratio is probably negligible except on the forward part of the body where the effect of lateral radius of curvature is small. Thus, although the results are restricted considerably thereby, the use of the three assumptions ( $\sigma = 1$ ,  $\delta = \Delta$ , and  $\frac{dT_w}{dx} = 0$ ) should reveal the salient features of the effect of lateral radius of curvature.

When these assumptions are used, the velocity and stagnation-temperature profiles are written

$$\bar{t} = \bar{w} = A_1 \eta_{*r} + A_2 (\eta_{*r})^2 + A_3 (\eta_{*r})^3 + A_4 (\eta_{*r})^4 \quad (A12)$$

where, with three asymptotic boundary conditions at the edge of the boundary layer,

$$\left. \begin{aligned} A_1 &= \frac{12 + \lambda'}{6} = \left( \frac{\partial w}{\partial \eta_{*r}} \right)_w = \left( \frac{\partial \bar{t}}{\partial \eta_{*r}} \right)_w \\ A_2 &= -\frac{\lambda'}{2} = \frac{1}{2} \left[ \frac{\partial^2 w}{\partial (\eta_{*r})^2} \right]_w = \left[ \frac{\partial^2 \bar{t}}{\partial (\eta_{*r})^2} \right]_w \\ A_3 &= \frac{3\lambda' - 12}{6} \\ A_4 &= \frac{6 - \lambda'}{6} \end{aligned} \right\} \quad (A13)$$



The expression for  $\lambda'$  is then obtained from either equation (A10) or (A11) as

$$\lambda' = \frac{-4 (\cos \beta_w) \frac{\Delta}{L}}{\frac{\cos \beta_w \Delta}{3} \frac{\Delta}{L} - \frac{\rho_w}{\rho^*_1} \left(\frac{r_w}{L}\right)^2} \quad (\text{A14})$$

for  $0 < \lambda' \leq 12$ .

Using equations (A12), (A13), and (A14) in the momentum equation (A8) gives

$$\frac{d\theta}{dx} = \frac{1}{18} \frac{\mu_w}{u_1 L \rho^*_1} \frac{(12 + \lambda')^2}{\lambda'} \quad (\text{A15})$$

for a circular cylinder ( $r_w$  being constant). The same result would, of course, be obtained from equation (A9) by using the assumptions discussed above. The value for  $\theta$  is obtained by integration of the expression

$$\theta = \Delta \int_0^1 \left( \frac{u}{u_1} - \frac{u^2}{u_1^2} \right) d\eta^*_r = \frac{\Delta}{315} \left[ 37 - \frac{\lambda'}{3} - \frac{5}{144} (\lambda')^2 \right]$$

Differentiating this equation and using equation (A14) for  $\Delta$  gives

$$\frac{d\theta}{dx} = \frac{3}{315} \frac{\rho_w}{\rho^*_1} \left(\frac{r_w}{L}\right)^2 \left[ \frac{37 - \frac{2}{3} \lambda' - \frac{15}{144} (\lambda')^2}{12 + \lambda'} - \frac{37\lambda' - \frac{(\lambda')^2}{3} - \frac{5}{144} (\lambda')^3}{(12 + \lambda')^2} \right] \frac{d\lambda'}{d\bar{x}} \quad (\text{A16})$$

for constant  $r_w$ . Equating (A15) and (A16) then gives a unique relation between  $\lambda'$  and  $\bar{x}$  as

$$d\bar{x} = \frac{6}{35} \left( \frac{r_w}{L} \right)^2 \frac{\rho_w u_1 L}{\mu_w} \left[ \frac{37\lambda' - \frac{2}{3}(\lambda')^2 - \frac{15}{144}(\lambda')^3}{(12 + \lambda')^3} - \frac{37(\lambda')^2 - \frac{(\lambda')^3}{3} - \frac{5(\lambda')^4}{144}}{(12 + \lambda')^4} \right] d\lambda' \quad (A17)$$

Integration of equation (A17) then results in

$$\xi^2 = \frac{\left( \frac{x}{r_w} \right)^2}{\frac{\rho_w u_1 x}{\mu_w}} = \frac{6}{35} \left\{ \frac{61}{72} - \frac{25}{288}(12 + \lambda') - \frac{23}{6(12 + \lambda')} + \frac{74 + \frac{(\lambda')^2}{6} + \frac{25}{864}(\lambda')^3}{(12 + \lambda')^2} + \left[ \frac{37}{3} - \frac{\lambda'}{9} - \frac{5}{432}(\lambda')^2 \right] \frac{(\lambda')^3}{(12 + \lambda')^3} + \frac{21}{12} [\log(12 + \lambda') - \log 12] \right\} \quad (A18)$$

Thus,  $\lambda'$  turns out to be a function only of the local body fineness ratio  $x/2r_w$  and the wall Reynolds number  $\frac{\rho_w u_1 x}{\mu_w}$ .

The local skin-friction coefficient is defined as

$$c_f = \frac{\mu_w \left( \frac{\partial u}{\partial y} \right)_w}{\frac{1}{2} \rho_1 u_1^2}$$

or transforming to  $\eta^*_r$  and using equations (A13) and (A14) results in

$$c_f = 4 \frac{\mu_w}{\rho_1 u_1 x} \frac{x}{r_w} \frac{1}{\lambda'} \left( \frac{12 + \lambda'}{6} \right)^2 \quad (A19)$$

The skin-friction coefficient for the flat plate with constant wall temperature is

$$c_{fP} = 2 \sqrt{\frac{37}{315}} \sqrt{\frac{\rho_w}{\rho_1} \frac{\mu_w}{\rho_1 u_1 x}}$$

and is derived from equation (50). Thus, forming the ratio of the skin-friction coefficient of the cylinder to that of the flat plate gives

$$\frac{c_f}{c_{f_p}} = 2 \sqrt{\frac{315}{37}} \frac{x/r_w}{\sqrt{\frac{\rho_w u_1 x}{\mu_w}}} \frac{1}{\lambda'} \left( \frac{12 + \lambda'}{6} \right)^2 = 2 \sqrt{\frac{315}{37}} \xi \frac{1}{\lambda'} \left( \frac{12 + \lambda'}{6} \right)^2 \quad (\text{A20})$$

where  $\lambda'$  is a function of  $\xi$  from equation (A18). Similarly, the local heat-transfer rate is

$$q_w = -k_w \left( \frac{\partial T}{\partial y} \right)_w$$

or transforming to  $\eta^*_r$  and using equations (A13) and (A14) give

$$q_w = -\frac{1}{18} k_w (T^*_1 - T_w) \frac{1}{r_w} \frac{(12 + \lambda')^2}{\lambda'} \quad (\text{A21})$$

The corresponding expression for the flat plate is

$$q_{w_p} = -\sqrt{\frac{37}{315}} k_w (T^*_1 - T_w) \sqrt{\frac{u_1 \rho_w x}{\mu_w}} \frac{1}{x}$$

since, with the assumptions used herein, namely,  $\sigma = 1$ ,  $\delta = \Delta$ , and  $\frac{dT_w}{dx} = 0$ , the temperature profile on the plate is

$$\frac{T}{T_1} = \frac{T_w}{T_1} - \frac{\gamma - 1}{2} M_1^2 \frac{2}{w^2} + \left( \frac{T^*_1}{T_1} - \frac{T_w}{T_1} \right)_w$$

(With the present assumptions, this same temperature profile also satisfies equations (A1) and (A3) for the slender cylinder.) The flat-plate relations from equations (12) and (40) with  $\lambda = 0$  and  $C_w$  constant have also been used to form  $q_{w_p}$ . Forming the ratio of  $q_w/q_{w_p}$  then results in

$$\frac{q_w}{q_{w_p}} = \frac{c_f}{c_{f_p}} \quad (A22)$$

The mean skin-friction coefficient is obtained by integrating equation (A19) from  $x = 0$  to  $x = L$  and using equation (A17) as the relation between  $d\bar{x}$  and  $d\lambda'$ . The result is

$$c_f = \frac{2}{105} \frac{r_w}{L} \frac{\rho_w}{\rho_1} \left[ 45 - \frac{12 + \lambda'}{3} - \frac{492}{12 + \lambda'} - \frac{5}{144} \frac{(\lambda')^3}{12 + \lambda'} \right]$$

The mean skin-friction coefficient on the flat plate is

$$c_{f_p} = 4 \sqrt{\frac{37}{315}} \sqrt{\frac{\rho_w}{\rho_1}} \frac{1}{\sqrt{\frac{\rho_1 u_1 L}{\mu_w}}}$$

The ratio of the mean skin-friction coefficient for the cylinder to that of the flat plate is

$$\frac{c_f}{c_{f_p}} = \frac{1}{210} \sqrt{\frac{315}{37}} \frac{r_w}{L} \sqrt{\frac{\rho_w u_1 L}{\mu_w}} \left[ 45 - \frac{12 + \lambda'}{3} - \frac{492}{12 + \lambda'} - \frac{5}{144} \frac{(\lambda')^3}{12 + \lambda'} \right] \quad (A23)$$

where  $\lambda'$  must correspond to the values from equation (A18) with  $x = L$ .

In figure 7, equations (A20) and (A23) are plotted against

$$\xi = \frac{x}{r_w} \sqrt{\frac{\mu_w}{\rho_w u_1 x}} \quad \text{which is similar to the parameter used by Seban and Bond-}$$

(ref. 25). The ratio  $c_f/c_{f_p}$  from reference 25 is plotted against

$$\xi' = \frac{x}{r_w} \sqrt{\frac{\mu_1}{\rho_1 u_1 x}} \quad \text{in figure 7.}$$

Figure 7 shows that the results from the present method are in good agreement with those from reference 25 if the stream Reynolds number  $\rho_1 u_1 x / \mu_1$  in reference 25 is replaced by the wall Reynolds number  $\rho_w u_1 x / \mu_w$ . The compressibility effect on the slender cylinder is thus approximately accounted for by evaluating the gas properties at the wall rather than in the free stream. This result might have been anticipated in view of a discussion in reference 27 on the compressibility effect in the laminar boundary layer.

The effects of the lateral radius of curvature on both the skin friction and heat transfer are increased over the incompressible effects in almost direct proportion to  $T_w/T_1$  since

$$\xi = \frac{T_w}{T_1} \xi'$$

with the present assumption for the viscosity variation. As a practical example, consider a body of fineness ratio 15 at  $M_1 = 5.00$  and  $R_{1L} = 2 \times 10^6$  with  $\frac{T_w}{T_1} = 5$ . Under these conditions the value of  $\xi_L$  at the rear of the body is

$$\xi_L = \frac{L/r_w}{\sqrt{\frac{\rho_w u_1 L}{\mu_w}}} = 0.11$$

( $\xi_L$  is the value of  $\xi$  where  $x = L$ .) Then, from figure 7 the local skin-friction and heat-transfer coefficients would be about 20 percent greater than those on a flat plate for the same stream conditions. The mean skin-friction coefficient and, incidentally, the total heat transfer would be about 7 percent greater than on the plate.

## REFERENCES

1. Thwaites, B.: Approximate Calculation of the Laminar Boundary Layer. *Aeronautical Quarterly*, vol. I, pt. III, Nov. 1949, pp. 245-280.
2. Truckenbrodt, E.: Ein Quadraturverfahren zur Berechnung der laminaren und turbulenten Reibungsschicht bei ebener und rotationssymmetrischer Strömung. *Ing.-Archiv*, Bd. XX, Heft 4, Aug. 1952, pp. 211-227.
3. Rott, Nicholas, and Crabtree, L. F.: Simplified Laminar Boundary-Layer Calculations for Bodies of Revolution and for Yawed Wings. *Jour. Aero. Sci.*, vol. 19, no. 8, Aug. 1952, pp. 553-565.
4. Morduchow, Morris, and Clarke, Joseph H.: Method for Calculation of Compressible Laminar Boundary-Layer Characteristics in Axial Pressure Gradient With Zero Heat Transfer. NACA TN 2784, 1952.
5. Dienemann, W.: Calculation of the Thermal Boundary Layer of a Body in Incompressible Laminar Flow. *Jour. Aero. Sci. (Readers' Forum)*, vol. 18, no. 1, Jan. 1951, pp. 64-65.
6. Morduchow, Morris: On Heat Transfer Over a Sweat-Cooled Surface in Laminar Compressible Flow With a Pressure Gradient. *Jour. Aero. Sci.*, vol. 19, no. 10, Oct. 1952, pp. 705-712.
7. Kalikhman, L. E.: Heat Transmission in the Boundary Layer. NACA TM 1229, 1949.
8. Van Driest, E. R.: Calculation of the Stability of the Laminar Boundary Layer in a Compressible Fluid on a Flat Plate With Heat Transfer. *Jour. Aero. Sci.*, vol. 19, no. 12, Dec. 1952, pp. 801-812.
9. Weil, Herschel: Effects of Pressure Gradient on Stability and Skin Friction in Laminar Boundary Layers in Compressible Fluids. *Jour. Aero. Sci.*, vol. 18, no. 5, May 1951, pp. 311-318.
10. Sternberg, Joseph: A Free-Flight Investigation of the Possibility of High Reynolds Number Supersonic Laminar Boundary Layers. *Jour. Aero. Sci.*, vol. 19, no. 11, Nov. 1952, pp. 721-733.
11. Gazley, Carl, Jr.: Boundary-Layer Stability and Transition in Subsonic and Supersonic Flow. A Review of Available Information With New Data in the Supersonic Range. *Jour. Aero. Sci.*, vol. 20, no. 1, Jan. 1953, pp. 19-28.

12. Chapman, Dean R., and Rubesin, Morris W.: Temperature and Velocity Profiles in the Compressible Laminar Boundary Layer With Arbitrary Distribution of Surface Temperature. Jour. Aero. Sci., vol. 16, no. 9, Sept. 1949, pp. 547-565.
13. Brown, W. Byron, and Donoughe, Patrick L.: Tables of Exact Laminar-Boundary-Layer Solutions When the Wall Is Porous and Fluid Properties Are Variable. NACA TN 2479, 1951.
14. Fluid Motion Panel of the Aeronautical Research Committee and Others: Modern Developments in Fluid Dynamics. Vol II, ch. XIV, sec. 270, S. Goldstein, ed., The Clarendon Press (Oxford), 1938, p. 631.
15. Goland, Leonard: A Theoretical Investigation of Heat Transfer in the Laminar Flow Regions of Airfoils. Jour. Aero. Sci., vol. 17, no. 7, July 1950, pp. 436-440.
16. Eber, G. R.: Experimentelle Untersuchung der Bremstemperatur und des Wärmeüberganges an einfachen Körpern bei Überschallgeschwindigkeit. Archiv Nr. 66/57, Peenemünde, Nov. 21, 1941. (Translation GTR #22 by Engineering Dept., Chance Vought Aircraft, May 20, 1946.)
17. Moore, L. L.: A Solution of the Laminar Boundary-Layer Equations for a Compressible Fluid With Variable Properties, Including Dissociation. Jour. Aero. Sci., vol. 19, no. 8, Aug. 1952, pp. 505-518.
18. Mangler, W.: Kompressible Grenzschichten an Rotationskörpern. Albert Betz zum 60. Geburtstag, Aerodynamischen Versuchsanstalt Göttingen und Kaiser Wilhelm Instituts für Strömungsforschung, Dec. 25, 1945.
19. Libby, Paul A., Morduchow, Morris, and Bloom, Martin: Critical Study of Integral Methods in Compressible Laminar Boundary Layers. NACA TN 2655, 1952.
20. Levy, Solomon: Heat Transfer to Constant-Property Laminar Boundary-Layer Flows With Power-Function Free-Stream Velocity and Wall-Temperature Variation. Jour. Aero. Sci., vol. 19, no. 5, May 1952, pp. 341-348.
21. Johnson, H. A., and Rubesin, M. W.: Aerodynamic Heating and Convective Heat Transfer - Summary of Literature Survey. Trans. A.S.M.E., vol. 71, no. 5, July 1949, pp. 447-456.
22. Eckert, E., and Weise, W.: Messungen der Temperaturverteilung auf der oberfläche schnell angeströmter unbeheizter Körper. Forsch. Geb. Ing.-Wes., Bd. 13, 1942, pp. 246-254.

23. Rott, N.: Compressible Laminar Boundary Layer on a Heat-Insulated Body. Jour. Aero. Sci. (Readers' Forum), vol. 20, no. 1, Jan. 1953, pp. 67-68.
24. Wimbrow, William R.: Experimental Investigation of Temperature Recovery Factors on Bodies of Revolution at Supersonic Speeds. NACA TN 1975, 1949.
25. Seban, R. A., and Bond, R.: Skin-Friction and Heat-Transfer Characteristics of a Laminar Boundary Layer on a Cylinder in Axial Incompressible Flow. Jour. Aero. Sci., vol. 18, no. 10, Oct. 1951, pp. 671-675.
26. Young, A. D.: The Calculation of the Total and Skin Friction Drags of Bodies of Revolution at Zero Incidence. R. & M. No. 1874, British A.R.C., 1939.
27. Tifford, Arthur N.: Simplified Compressible Laminar Boundary-Layer Theory. Jour. Aero. Sci. (Readers' Forum), vol. 18, no. 5, May 1951, pp. 358-359.



TABLE I.- NUMERICAL VALUES OF  $\alpha$  FOR EQUATION (35)

Thermal profile			$\alpha$	$\alpha_1$	$\alpha_2$	$\alpha_3$	$\alpha_4$	$\alpha_5$	$\alpha_6$	$\alpha_7$
Degree of polynomial	Number of boundary conditions									
	Wall	Edge								
5	2	2	0.381746	-0.146032	-0.053175	-0.013889	0.044841	-0.012302	-0.003572	-0.000794
6	2	3	.29805	-.09582	-.028067	-.00552	.041234	-.010137	-.002489	-.000433
4	0	3	.17381	-.028175	0	0	.029762	-.003968	0	0
4	1	2	.326190	-.104365	-.025397	0	.041667	-.009921	-.001984	0
5	1	3	.24286	-.062698	-.011508	0	.036905	-.007540	-.001190	0
6	1	4	.187662	-.040625	-.005988	0	.032576	-.005808	-.000758	0



Relative heat-transfer values with $\frac{dT_w}{dx} = 0; n = 0$					Degree of thermal profile	Number of boundary conditions	
Description of thermal profile			$Y_n'(0)$	Percent error		Wall	Edge
Degree of polynomial	Number of conditions at wall	Number of conditions at edge					
4	0	3	0.543	-8.2	□	2	1
4	1	2	.601	1.6	○	2	2
5	1	3	.577	-2.5	◇	2	3
6	1	4	.526	-11.1	□	0	3
4	2	1	.541	-8.5	▽	1	4
5	2	2	.575	-2.8	▷	1	3
6	2	3	.576	-2.6	△	1	2
Exact, ref. 12			0.5915	0			

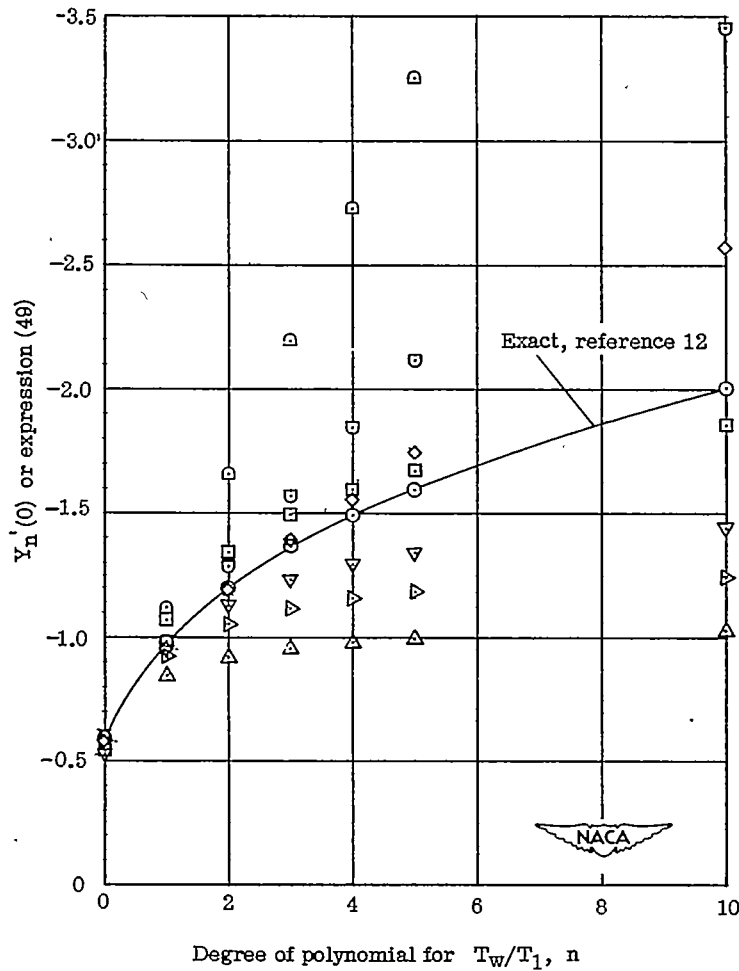


Figure 1.- Variation of heat-transfer parameter with  $n$  for the non-isothermal flat plate with  $\sigma = 0.72$ . The symbol  $n$  is defined by

the equation 
$$\frac{T_w}{T_1} = \frac{T_e}{T_1} + \sum_{n=0}^{\infty} a_n x^{-n}.$$

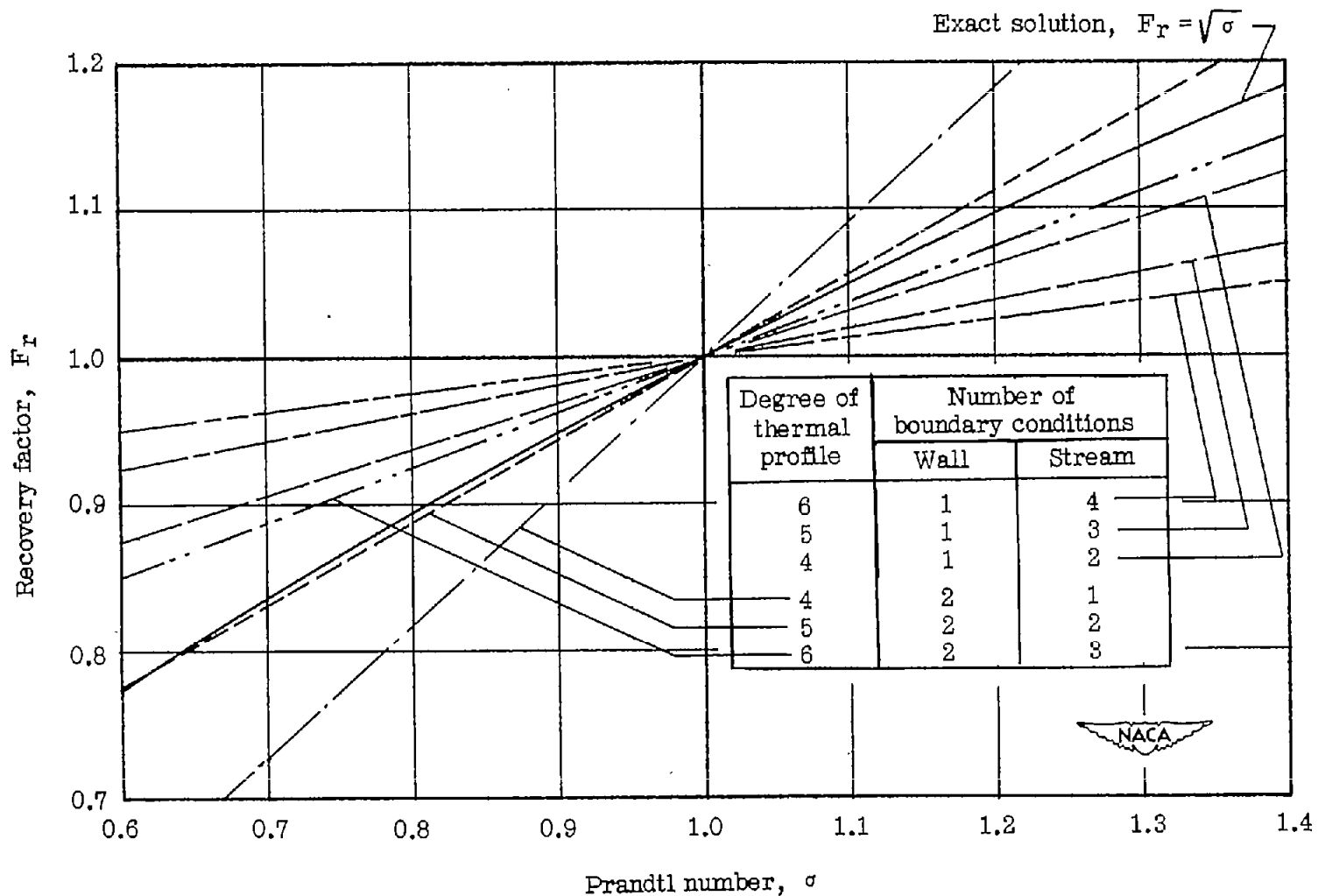


Figure 2.- The recovery factors on a flat plate obtained by various stagnation temperature profiles from the present method and the exact values given by  $F_r = \sqrt{\sigma}$ .

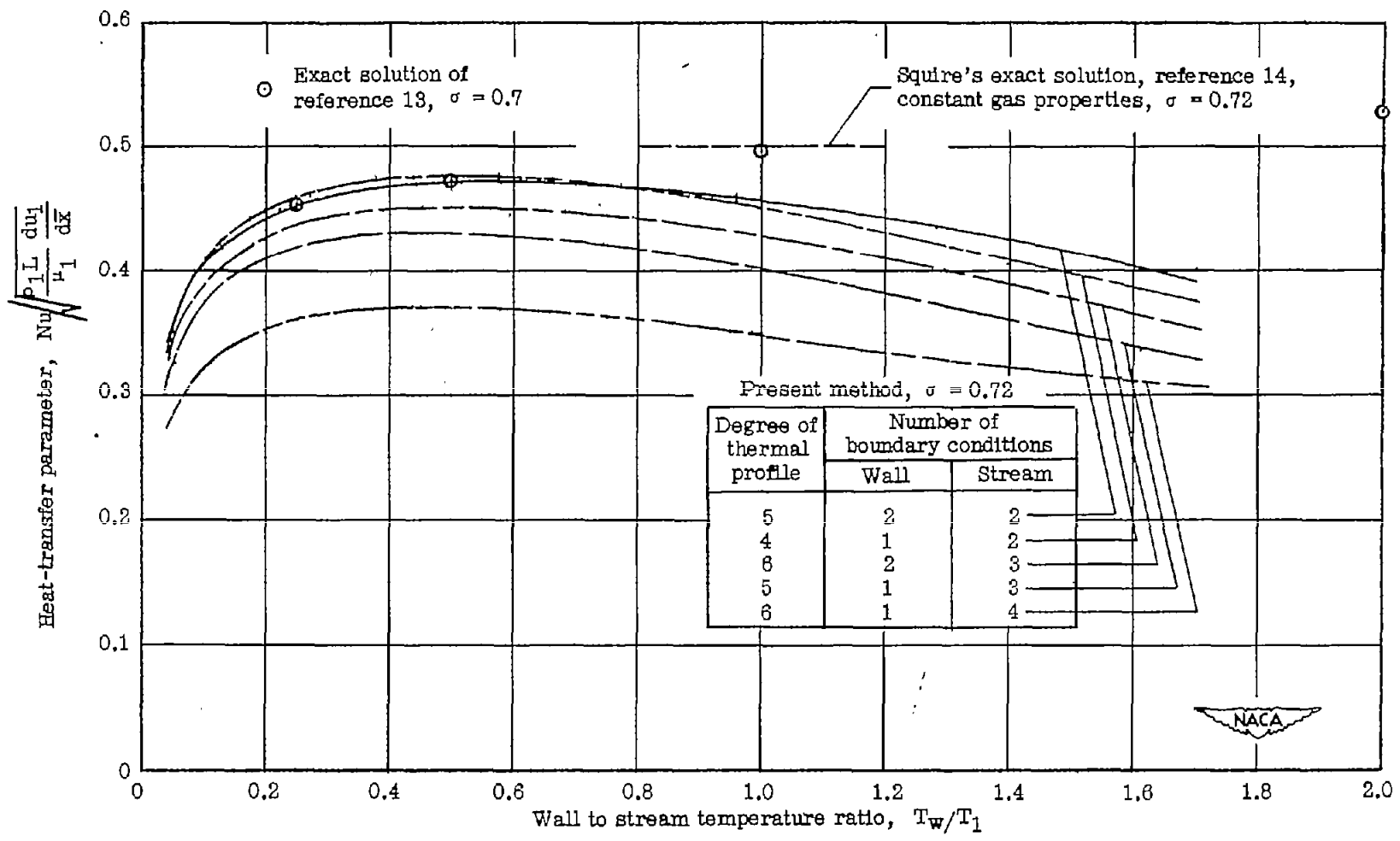


Figure 3.- Variation of heat-transfer parameter with the ratio of wall to local stream temperature for the stagnation region of a blunt body.  
 $T^*_1 = 500^\circ \text{ R.}$

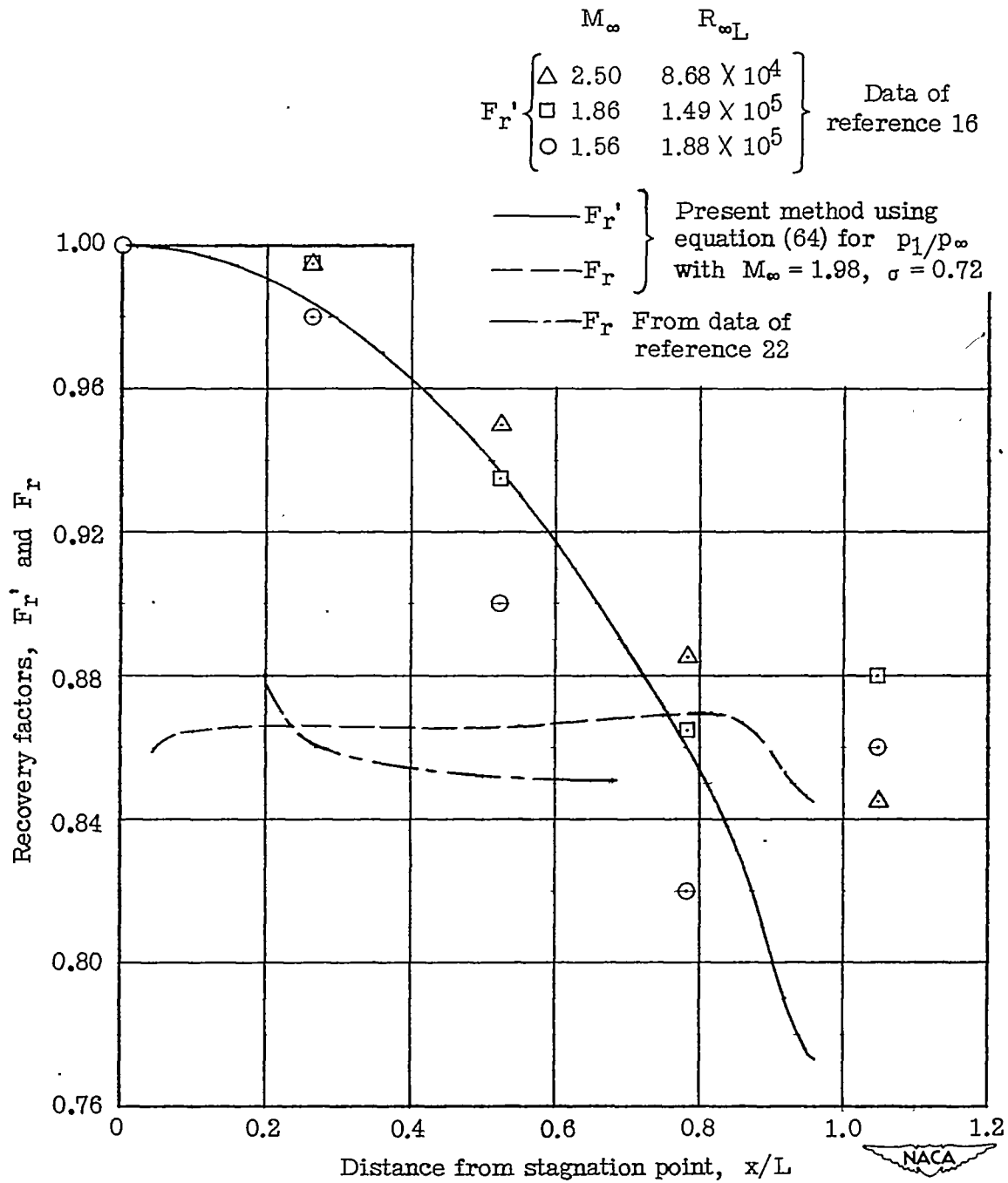


Figure 4.- Local free-stream recovery factor  $F_r'$  and local recovery factor  $F_r$  on a circular cylinder with axis normal to the flow. Separation occurs at approximately  $\frac{x}{L} = 1.0$  where  $L$  is the cylinder diameter.

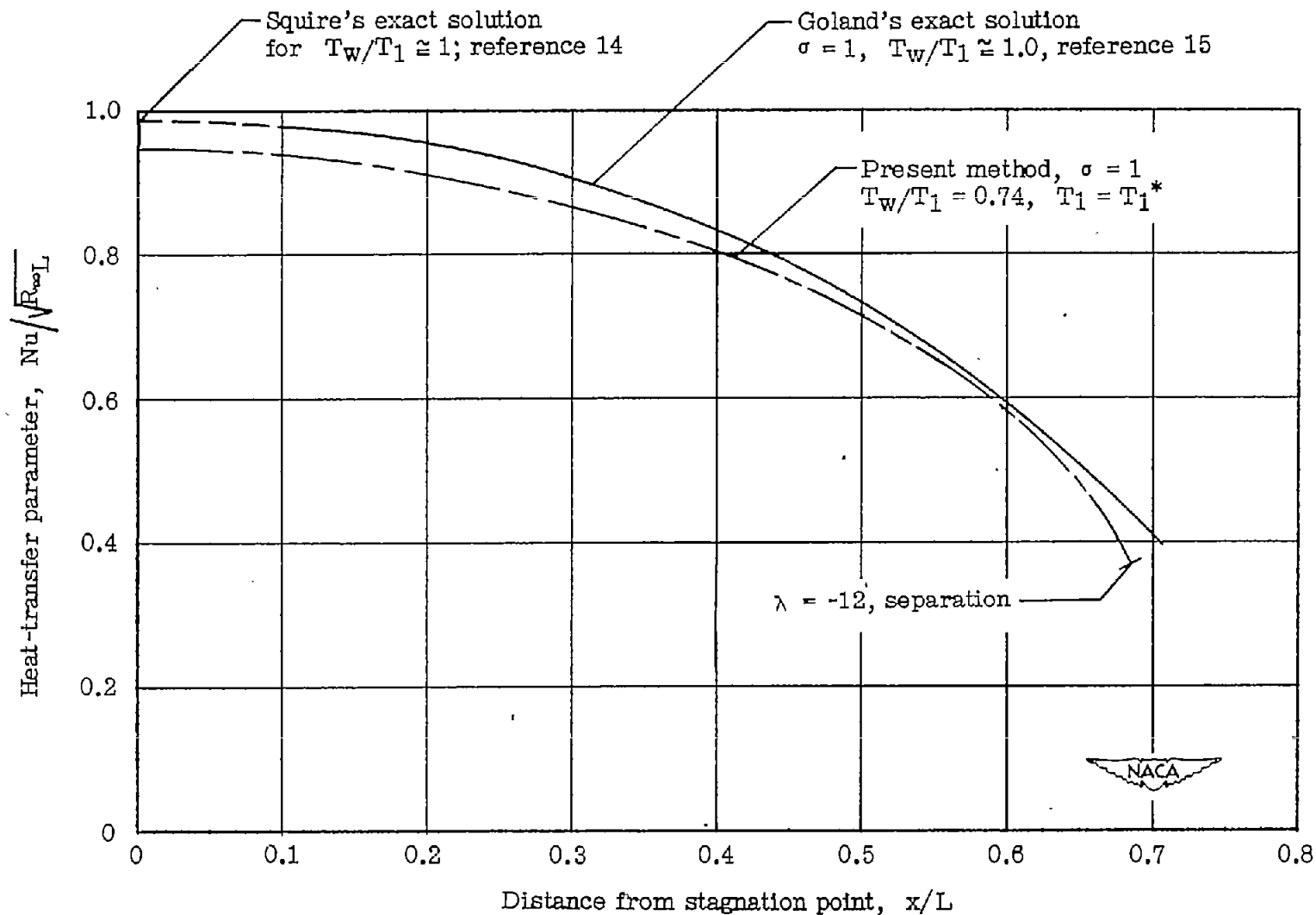


Figure 5.- Heat transfer on a cylinder by the present method and from Goland's exact solution.

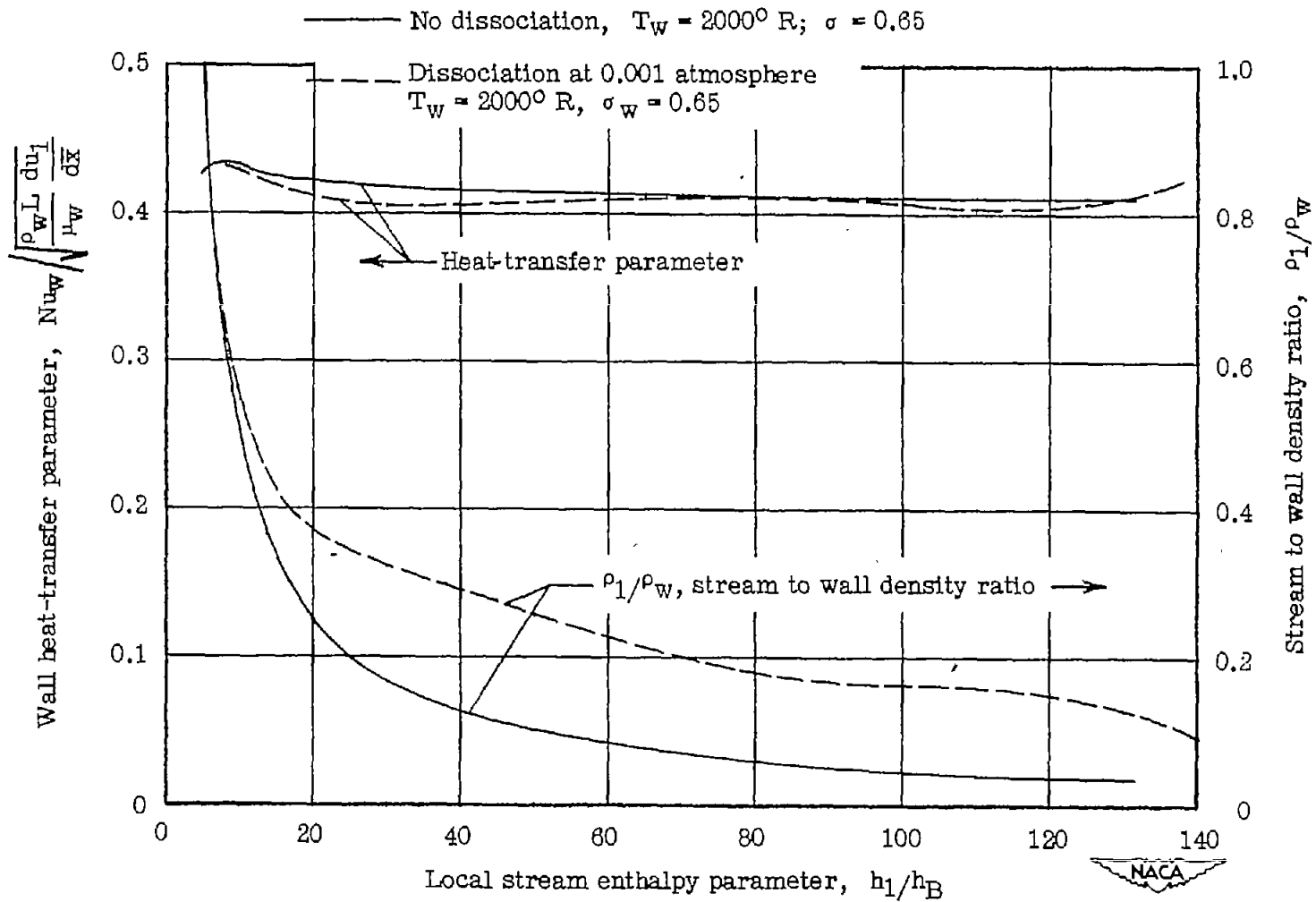


Figure 6.- Variation of heat-transfer parameter with stream enthalpy parameter with and without dissociation at the stagnation point of a blunt body. Wall temperature,  $T_W = 2,000^\circ \text{ R}$ .

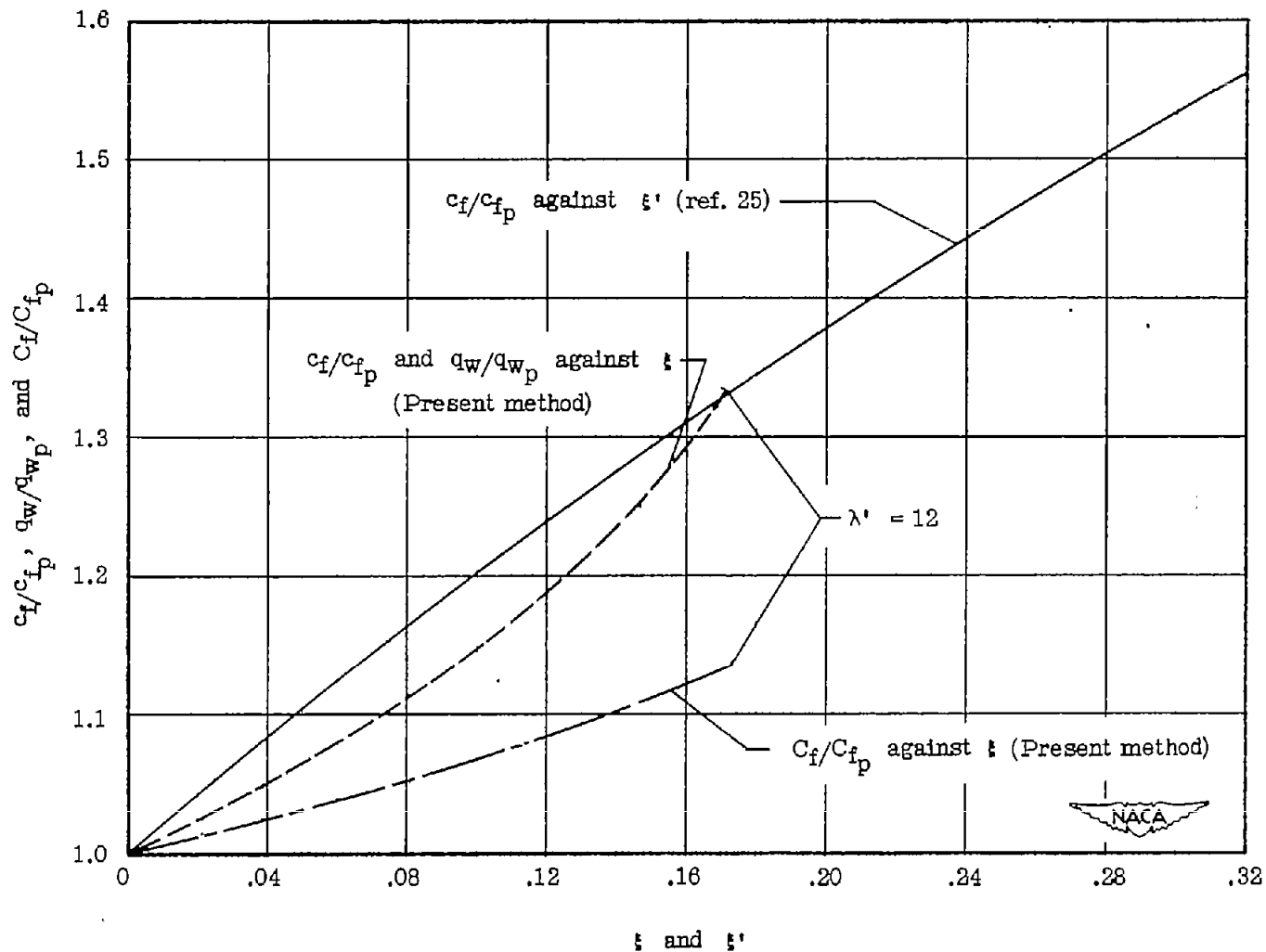


Figure 7.- The ratio of skin-friction and heat-transfer coefficients on a slender cylinder to the corresponding coefficients on a flat plate. The subscript "p" denotes the flat-plate values.